2024, 21(3): 0867-0893
https://dx.doi.org/10.21123/bsj.2023.8382
P-ISSN: 2078-8665 - E-ISSN: 2411-7986
Baghdad Science Journal

Spatial Distribution of Heavy Element in Erbil's Municipal Landfills by Using GIS

Sayran Yousif Jalal** *, **Dalshad Azeez Darwesh

Department of Environmental Science and Health, College of Science, University of Salahaddin, Erbil, Iraq.
*Corresponding Author.

Received 17/01/2023, Revised 24/02/2023, Accepted 26/02/2023, Published Online First 20/08/2023, Published 01/03/2024

Abstract

Untreated municipal solid waste (MSW) release onto land is prevalent in developing countries. To reduce the high levels of harmful components in polluted soils, a proper evaluation of heavy metal concentrations in Erbil's Kani Qrzhala dump between August 2021 and February 2022 is required. The purpose of this research was to examine the impact of improper solid waste disposal on soil properties within a landfill by assessing the risks of contamination for eight heavy elements in two separate layers of the soil by using geoaccumulation index (I-geo) and pollution load index (PLI) supported. The ArcGIS software was employed to map the spatial distribution of heavy element pollution and potential ecological risks. The I-geo values in summer varied from -1.700 to 3.560 for Zn, 5.045 to 8.175 for Cd, 2.318 to 4.329 for Pb, 0 to 3.374 for Mn, 1.439 to 3.880 for Ni, 0.638 to 2.278 for Cu, -0.541 to 2.665 for Cr, and -2.495 to 0.778 for Hg. Based on the I-geo categorization, the contamination levels of Zn, Cd, Pb, Mn, Ni, Cu, and Hg ranged from uncontaminated to extremely contaminated. However, all metals were assessed as uncontaminated throughout winter, except I-geo (Cd) and I- geo (Ni) varied from -0.467 to 3.966 and -5.720 to 2.015 were classified from as uncontaminated to strong and uncontaminated to moderately/strongly contaminated respectively. According to the PLI category, most samples were rated as "highly polluted" during summer, but during the rainy season, all samples were rated as "unpolluted".

Keywords: Geoaccumulation Index, GIS, Heavy elements, MSW, PLI.

Introduction

Heavy element contamination of soil has received significant environmental focus in recent years. Industry, coal and fuel burning, and car emissions, mining operations, use of fertilizers and pesticides, municipal solid waste disposal, and other activities are the sources of trace element releases into the soil, particularly urban soils [1, 2].

In developing countries, ineffective solid waste management is a significant issue. So, the ecosystem has become contaminated with potentially hazardous substances. The absence of a clear approach for source segregation can intensify contamination of the environment. Waste disposal has emerged as an essential component of integrated solid waste management when considering sustainable development goals. Landfilling is the most popular method for disposing of various solid wastes worldwide [3].

The geochemical characteristics of agricultural soils, especially the concentrations of heavy elements, determine the quality of the soil [4, 5]. Accumulation of heavy elements may endanger humans and natural systems via exposure to polluted soil or food, Phytotoxicity endangers the food chain (plant-soil-human), pollutes groundwater, and degrades food quality (safety and commercial viability), and declining soil use for crop output, resulting in food shortages and communal land issues [6].

Crop development requires the frequent application of substantial volumes of nitrogen, phosphorus and potassium fertilizers in modern agricultural practices. Compounds containing trace amounts of these elements, but when applied continuously in the form of fertilizers, they can greatly enhance the soil mineral composition [7].

In addition, heavy elements such as nickel, boron, cadmium, lead, arsenic, cobalt, and chromium make significant health risks to humans, animals, and vegetation. Ni, for instance, promotes plant growth, but excessive Ni can increase likelihood to both humans and other animals. But presence of too much Ni within soil can raise the probability of skin, nose, and lung cancers[8].

Soil pollution causes foundation failure, land subsidence, landslides, contamination of groundwater quality, etc. Therefore, it is crucial to understand the contamination properties of soils to guarantee the integrity of structural components and inhibit the failure of existing structures[9].

Physical, chemical, index, and engineering properties can be used to deduce the contamination characteristics of the soil. The manual processes of spatial model evaluation, interpolation, and generation are difficult and time-consuming. GIS can be useful in such situations. Because of the rapid development of GIS applications in fields such as contamination, noise pollution, commercial and utility GIS, and so on, in which data is gathered in discrete form, interpolation methods can be employed to acquire continuous data [10].

Globalization and unregulated agricultural activities have altered natural landscapes and ecosystems [11]. Hence, the assessment of soil contamination must take into account a deep understanding of the spatial distribution of contaminants [12].

A GIS database would provide comprehensive information for low-cost soil monitoring[13]. heavy elements distribution and concentration must be analyzed. This will allow the determination of pollutant levels and the evaluation of their effects on the environment and human health. Soil toxic element analysis and mapping can aid in the development of strategies that encourage the appropriate utilization of soil nutrients, decrease soil degradation, and increase agricultural output. Soil pollutants are surveyed and their spatial distributions are analyzed using geophysical survey [14]. The Kriging function is helpful for assessing pollution levels comprehensively [15]. To reduce the excessive concentrations of toxic components in polluted soil, precise estimation of toxic element concentrations in soils, backed by GIS database systems, is necessary [16].

So, the objectives of this study were to (i) map soil contamination based on three heavy elements (Cd, Pb, and Ni) using (GIS) in 26 soil sites and two soil layers; and (ii) evaluate the possible contamination for eight heavy elements using I-geo and PLI in two distinct soil strata.

The Study Area

The study area is located north of Kani Qrzhala Sub District Fig. 1 in Erbil City, on the left side of Erbil-Mosul major road, Iraq. The location's longitude and latitude belong to (latitudes 36°10'23" north and longitudes 43°35'32" east; Fig. 1). In which, the landfill, began operations in 2001, covers an area of 37 acres. The vast bulk of the landfill area has already been occupied. The location gets almost 2000 t of municipal solid waste every day (based on data collected from ELS administrative staff). The waste is transported into landfills, which are then filled without separation and covered with layers of soil. The site was selected because it is now used as a rubbish dump and septic tank discharge region, highlighting the environmental repercussions that are developing.

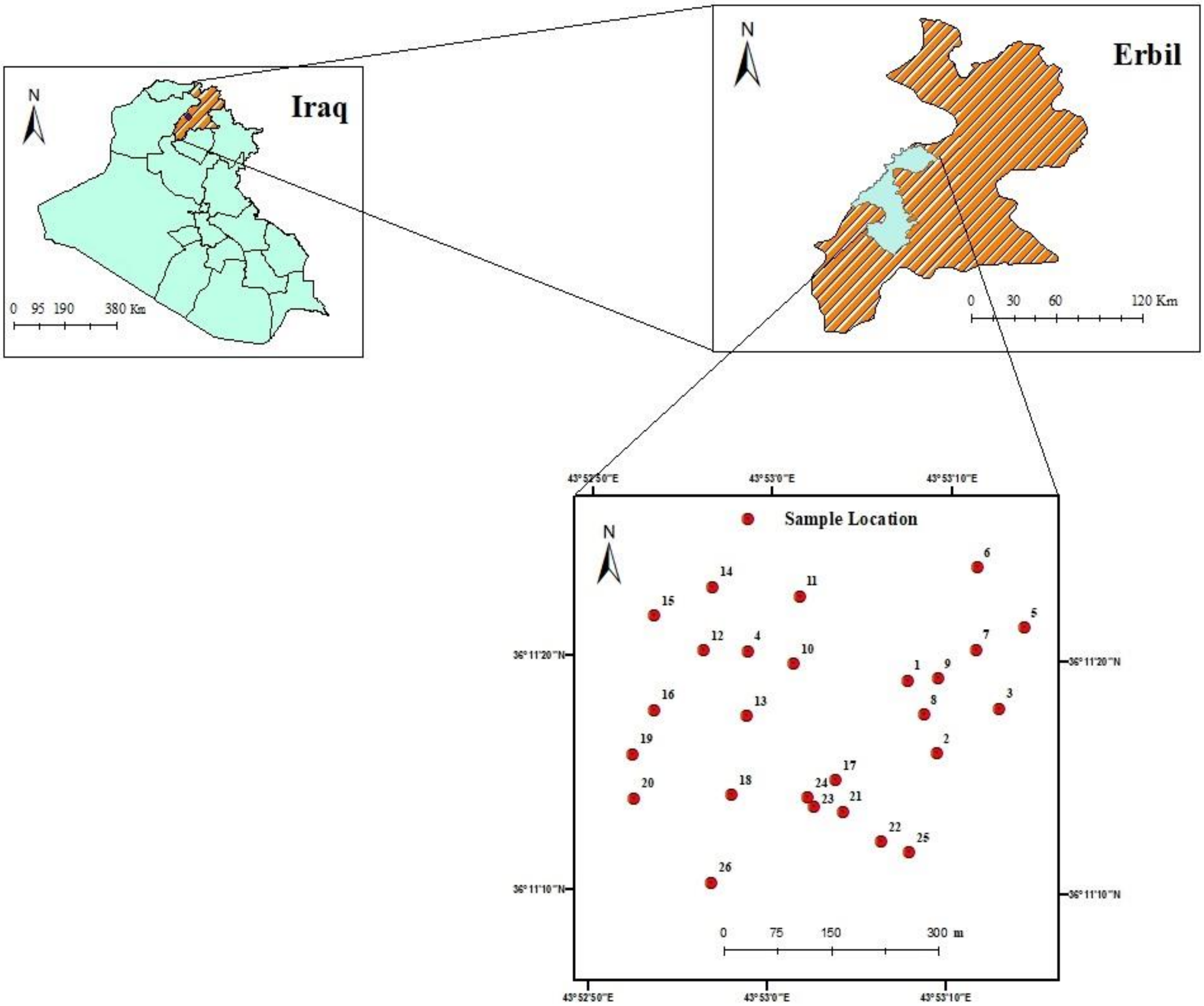

Figure 1. Study area location and sites of sample collection.

Materials and Methods

Soil Analysis:

Samples of soil were collected from 26 representative sites in Erbil's Kani Qrzhala sub-districts between August 2021 and February 2022. Soil sites were selected on the basis of local geological characteristics to show how the different landfill processes work. Different layers of soil were sampled depending on their distinct shapes. Since each physiographic unit encompasses contains multiple profiles, the level of certainty in the distribution is high due to the extensive coverage of the physiographic units. As illustrated in Fig. 1, the investigated profiles and soil sample sites were ascertained utilizing a Global Positioning System (GPS) unit German-made.

Soil samples were gathered from the preferred top layers. Because there are no morphological variations in the soil profiles in the investigation area, soil samples were taken at two depths. At levels of, 0–5 cm and 5–30 cm, two soil samples were obtained from each profile and collecting soil samples was at summer and winter. All samples were packed in plastic bags and returned to the lab. The samples were composited, homogenized, dried at temperatures ranging from 25 - 35 degrees Celsius, crushed, and sieved to 2 mm[17].

Aqua regia (EDTA 0.05M) was used to take a sample of 5 g of powdered soil to determine element concentration. The concentration of Zn, Cd, Pb, Mn, Ni, Cu, Cr, and Hg was measured by an atomic absorption spectrometer (Atomic Absorption Spectrometer, Perkins Elmer, USA 1100D). Furthermore, heavy elements levels in soil were compared to threshold levels in mg kg^{-1} dry soil [18].

GIS Application:

Throughout this investigation, GPS was used to obtain data from Erbil and coordinate points. Every location's latitude and longitude were recorded, and all received data were processed using ArcGIS version 10.8 from [2]. The Kriging interpolation method software was used to calculate the intensity of each of the three heavy elements (Cd, Pb, and Ni). Kriging produces a satisfactory outcome when the points are distributed uniformly and a significant number of elevation points exist in a particular region. Furthermore, sample points are assumed to be independent of one another [19, 20]. Interpolation is typically used to forecast cell values in a pattern format using a given number of sample data points. It is a useful technique for predicting unknown values for a specific set of geographical location information.

Assessment of Contamination:
Geoaccumulation Index (I-geo)

The I-geo reflects contamination by comparing heavy elements levels determined with background values previously used to evaluate bottom sediments [21]. The geographic accumulation index (I-geo) was used to measure heavy elements contamination with the following Eq. 1:

$$Igeo = Log_2 \frac{Cn}{1.5\ Bn} \qquad \text{….1}$$

where Cn is the observed concentration of heavy element in the soil and Bn is their geochemical background concentration (medium crust) [22]. To limit the impact of any changes in threshold values that might be attributable to variations in sedimentary rocks, the constant 1.5 was included in Eq 1. Although soil is a component of the earth's surface and its chemical structure is related to that of the crust, this concentration falls between the concentration observed and that of the elements in the crust [23]. Table 1 depicts the I-geo classification.

Table 1. Class, value, and contamination level determined by geoaccumulation index (I-geo) in soil [23].

I-geo Class	I-geo Value	Contamination Level
0	I-geo ≤ 0	Uncontaminated
1	0 < I-geo < 1	Uncontaminated/moderately contaminated
2	1 < I-geo < 2	Moderately contaminated
3	2 < I-geo < 3	Moderately/strongly contaminated
4	3 < I-geo < 4	Strongly contaminated
5	4 < I-geo < 5	Strongly/extremely contaminated
6	5 < I-geo	Extremely contaminated

The Pollution Load Index (PLI)

The PLI is a geometric mean of impurity coefficients (Cif) that characterizes the donation of all heavy metals in a given location [24]. The contamination factor (CF) was calculated by dividing the heavy element content by the reference value using the following Eq 2 [25]:

$$CF = \frac{Cn}{Bn} \qquad \text{….2}$$

The following Eq 3 was employed to construct the pollution load index (PLI), which is used to evaluate element contents in soils in relation to the background level [26]:

$$PLI = (CF_1 * CF_2 * \ldots * CFn)^{1/n} \qquad \text{….3}$$

Where CF represents the contamination factor and n represents the total number of elements.

2024, 21(3): 0867-0893
https://dx.doi.org/10.21123/bsj.2023.8382
P-ISSN: 2078-8665 - E-ISSN: 2411-7986
Baghdad Science Journal

This variable can be employed to assess the degree of environmental contamination in addition to improving and observably enhancing the quality of the soil. The classification of PLI is displayed in Table 2.

Table 2. Class, value, and pollution level based on pollution load index (PLI) in soil[26].

PLI Class	PLI Value	Pollution Level
1	$0 < PLI \leq 1$	Unpolluted
2	$1 < PLI \leq 2$	Moderately polluted to unpolluted
3	$2 < PLI \leq 3$	Moderately polluted
4	$3 < PLI \leq 4$	Moderately to highly polluted
5	$4 < PLI \leq 5$	Highly polluted
6	$5 \leq PLI$	Very highly polluted

Statistical Analysis:
The Statistical Package for Social Sciences (SPSS) software was applied to data analysis, descriptive analyses, and analysis of variance two-way ANOVA (ANOVA version 16), least square differences (LSD), and Duncan multiple range test (DMRT), and regression analysis at a significance level of $P<0.05$.

Results and Discussion

The Variation of Eight Heavy Metals in Two Different Layers of Soil:
In this study, contamination with Zn, Cd, Pb, Mn, Ni, Cu, Cr, and Hg was examined in two distinct soil layers, during summer and winter. In summer, the zinc concentration at the landfill site was between 32,312 to 1,238,230 mg kg $^{-1}$. Statistically, there were significant differences $p <0.05$ between the Zn concentrations at the down site, landfill site, and top site. As predicted, the maximum concentration of Zn metal was found at the landfill's down-site location, with a value of 1238.230 mg kg $^{-1}$, while the lowest concentration was found at the top-site (32.312 mg kg $^{-1}$). The existence of Zn within the landfill site could be related to heavy element disposal, which also contains the dry cells and the combustion of electrical waste[27]. Zn is a micronutrient that plays an important role in enzymatic processes, and its availability in the soil can result in decreased Cd uptake by plants [28]. Even if the Zn content exceeded the allowable concentration level, excessive consumption may be harmful to human health.

Cadmium is an infrequent heavy element, but it is the most harmful heavy element to human health [29]. Cadmium concentrations were found to be significantly different $p <0.05$ between sampling sites in this study, Table 3. The lowest Cd content was 20.165 mg kg $^{-1}$ and the highest concentration was 177.715 mg kg $^{-1}$ of the metal, Table 3. The significant amount of Cd at the research location during the summer could be attributed to large intakes of cadmium-containing compounds from sludge, batteries, PVC (poly vinyl chloride) equipment, surface coatings, and vehicle lubricants [30].

Lead is regarded as a dangerous heavy element and has adverse effects on humans when swallowed [31]. Pb disrupts severely the water balance, enzyme activity, and mineral nutrition in greater amounts. Pb concentrations at several sampling sites varied significantly $p < 0.05$ and ranging from 201.89 to 813.81 mg kg $^{-1}$. Pb was found in the studied area due to the disposal of waste materials usually containing batteries, food packaging, PVC equipment, and insect repellents [32]. The maximum

Pb contents were found at site 13, indicating that the element is highly mobile Table 4.

Mn varied from 731.971 to 7589.760 mg kg^{-1}, the accumulation of Mn could be attributable to the careless dumping of solid waste and the introduction of leachate into the soil. Furthermore, a high concentration of manganese might be the result of garbage containing dry cell batteries, paints, glasses, and ceramics that were dumped at the landfill sites, as well as contamination from manganese dioxide cells, for which the city has no regulated disposal techniques [33].

The mean Ni concentrations varied from 117.927 to 640.340 mg kg^{-1} in landfill soils were greater than at the background level Table 5. Nickel is a harmful element typically found in leachate from hazardous waste landfills. It is generated through metal finishing, electroplating, organic waste, and the combustion waste of fossil fuels[34]. The existence of Ni in soils near the landfill may reveal that it did receive some industrial waste. There were considerable differences in Ni content between different layers at $p < 0.05$.

Cu concentration varied from 90.804 to 283.024 mg kg^{-1}. Both [35] and [36] elevated levels of Cu were discovered in the soils surrounding landfills. Copper is utilized in the production of numerous goods, such as wires, automotive components, pipelines, and alloy wheels that end up in landfills.

Chromium is an essential trace element for human health and well-being. Chromium pollution is a significant environmental threat that has negative effects on our surroundings and natural resources, particularly soil and water. Overexposure may lead to increased accumulation in human and animal tissues, resulting in toxic and negative health impacts. Several studies have found that chromium is a poisonous substance that interferes with plant metabolic processes, reducing crop yield and growth and decreasing grain and vegetable quality [37]. Cr varied from 261.797 to 566.048 mg kg^{-1}.

Hg ranged from 0.133 to 1.286 mg kg^{-1}, Tables. 3, 4, 5, and 6 along the two different layers in summer, the elevated levels of mercury associated with nearly three-quarters of the mercury in municipal solid waste come from battery packs and fluorescent lighting, which are expected to continue to be major mercury sources in the near future. Reduced or eliminated mercury levels in household items, especially batteries and fluorescent lights, ought to be the primary concern in mercury control in municipal solid waste, whereas mercury concentrations in consumer goods must also be set at appropriate and attainable levels using a life-cycle approach [38].

In contrast, the low amount of heavy elements in the soil during the winter months is a result of heavy elements infiltrating the soil even during the cold season[39], the Zn ranged from 9.021 to 138.788 mg kg^{-1}, Cd ranged from 0.445 to 9.611 mg kg^{-1}, Pb ranged from 12.418 to 73.303 mg kg^{-1}, Mn ranged from 1.014 to 175.829 mg kg^{-1}, Ni ranged from 0.240 to 8.373 mg kg^{-1}, Cu ranged from 0.743 to 101.476 mg kg^{-1}, Cr ranged from 4.717 to 12.547 mg kg^{-1} and Hg ranged from 0.005 to 0.038 mg kg^{-1} Tables 7, 8, 9 and 10 all over the two different layers.

In accordance with the research findings, all heavy elements were greater than permissible limits during summer, with the exception of Hg, which was within permissible limits in several sites. heavy elements in solid waste are mostly made up of toxic waste, such as batteries, paints, and inks [40]. As a result, the amounts of heavy elements are much lower in winter than in summer because the unequal slope and wet climate of our landfill encourage drainage and leaching of heavy elements by rainwater, resulting in lower percentages. Nevertheless, concentrations of heavy elements in household waste are lower than in industrial waste [41]. According to [42], the majority of heavy elements existing in soils contaminated by household solid waste could be removed through runoff, draining out, and infiltration.

2024, 21(3): 0867-0893
https://dx.doi.org/10.21123/bsj.2023.8382
P-ISSN: 2078-8665 - E-ISSN: 2411-7986
Baghdad Science Journal

Table 3. Standard deviation (SD) of (Zn and Cd) and Means (mg kg, Dry Weight) of study soil samples the same row followed by different letters are significantly different at $p < 0.05$ during summer.

Parameters	Zn				Cd			
Depth	**0-5 cm**		**5-30 cm**		**0-5 cm**		**5-30 cm**	
Sites	**Mean**	**SD**	**Mean**	**SD**	**Mean**	**SD**	**Mean**	**SD**
1	172.291[a]	0.353	1238.230[a]	35.378	176.890[ab]	35.378	26.533[ab]	1.061
2	265.335[abcd]	3.537	229.957[abcd]	12.755	50.826[b]	3.543	48.114[b]	2.151
3	126.299[bcd]	4.863	94.341[bcd]	4.085	20.165[b]	3.537	50.944[b]	3.537
4	265.335[bcd]	30.226	200.357[bcd]	12.971	100.827[ab]	33.317	92.926[ab]	2.702
5	153.305[cd]	54.040	147.526[cd]	1.969	58.138[ab]	11.031	56.015[ab]	12.257
6	600.247[abcd]	23.555	169.814[abcd]	20.846	57.077[ab]	15.719	50.826[ab]	7.432
7	181.607[bcd]	24.205	196.584[bcd]	6.696	128.304[ab]	18.854	29.246[ab]	1.472
8	401.069[abcd]	36.790	170.286[abcd]	16.267	57.077[ab]	15.719	125.002[ab]	39.570
9	381.139[abcd]	17.282	216.985[abcd]	35.732	61.912[b]	11.337	30.661[b]	3.896
10	707.560[abcd]	35.378	180.428[abcd]	14.621	42.925[b]	3.343	54.836[b]	17.486
11	365.337[ab]	39.460	664.988[ab]	48.695	46.345[ab]	0.612	92.808[ab]	15.340
12	821.595[ab]	27.973	306.845[ab]	15.743	65.803[ab]	10.441	65.213[ab]	12.903
13	273.354[abcd]	21.230	297.647[abcd]	23.627	63.091[ab]	21.392	66.393[ab]	34.007
14	384.323[abcd]	56.210	237.622[abcd]	49.123	34.906[b]	7.457	55.897[b]	22.467
15	412.154[abcd]	29.554	112.620[abcd]	34.377	62.265[ab]	19.260	70.756[ab]	35.378
16	730.084[abcd]	30.032	197.173[abcd]	42.341	58.610[ab]	19.108	47.053[ab]	20.528
17	769.000[abc]	68.196	278.071[abc]	53.329	42.100[ab]	20.177	117.927[ab]	54.040
18	625.438[abcd]	56.859	155.309[abcd]	57.080	104.247[ab]	62.112	76.299[ab]	36.086
19	348.237[abcd]	55.718	138.918[abcd]	61.771	93.752[ab]	28.406	151.064[ab]	60.970
20	213.211[abcd]	10.358	220.887[abcd]	29.455	177.715[a]	59.267	121.936[a]	50.714
21	469.112[abcd]	65.661	260.972[abcd]	26.442	90.568[ab]	48.102	64.388[ab]	21.785
22	698.362[abcd]	28.662	258.849[abcd]	36.252	170.876[ab]	54.659	76.063[ab]	15.384
23	625.011[abc]	54.040	411.092[abc]	35.285	76.416[ab]	34.675	116.747[ab]	37.867
24	691.876[abcd]	78.609	293.873[abcd]	36.364	127.715[ab]	35.773	98.940[ab]	44.538
25	655.672[abcd]	57.313	264.392[abcd]	28.446	71.228[ab]	11.166	36.203[ab]	6.678
26	32.312[d]	2.484	72.053[d]	20.768	87.502[ab]	30.310	70.284[ab]	21.826

2024, 21(3): 0867-0893
https://dx.doi.org/10.21123/bsj.2023.8382
P-ISSN: 2078-8665 - E-ISSN: 2411-7986
Baghdad Science Journal

Table 4. Standard deviation (SD) of (Pb and Mn) and Means (mg kg^{-1}, Dry Weight) of study soil samples the same row followed by different letters are significantly different at $p < 0.05$ during summer.

Parameters	**Pb**				**Mn**			
Depth	**0-5 cm**		**5-30 cm**		**0-5 cm**		**5-30 cm**	
Sites	**Mean**	**SD**	**Mean**	**SD**	**Mean**	**SD**	**Mean**	**SD**
1	680.319^{ab}	0.707	337.152^{ab}	3.374	1323.727^{e}	20.324	1999.918^{e}	11.501
2	339.747^{b}	4.816	205.310^{b}	36.352	1713.946^{bcde}	3.896	4941.127^{bcde}	167.189
3	273.236^{b}	19.417	234.438^{b}	18.788	3341.098^{bcde}	65.359	1712.413^{bcde}	200.207
4	306.963^{b}	30.518	278.071^{b}	22.617	3010.904^{bcde}	32.021	3548.767^{bcde}	35.556
5	284.439^{b}	34.670	287.269^{b}	35.378	1706.635^{de}	34.675	2227.989^{de}	87.056
6	303.307^{b}	32.163	318.992^{b}	28.915	3244.163^{bcde}	49.209	2244.027^{bcde}	34.342
7	370.172^{ab}	23.531	324.298^{ab}	25.016	900.724^{e}	30.957	1997.560^{e}	36.653
8	490.693^{ab}	16.514	433.970^{ab}	41.499	3514.097^{bcde}	34.534	2880.595^{bcde}	29.591
9	479.372^{ab}	30.949	284.911^{ab}	35.555	3557.730^{cde}	58.557	1298.491^{cde}	74.728
10	288.449^{b}	36.439	358.143^{b}	37.536	3160.553^{bcde}	31.667	2925.298^{bcde}	82.503
11	288.920^{ab}	33.609	387.153^{ab}	20.076	3903.373^{bcde}	54.040	2496.743^{bcde}	20.599
12	287.859^{b}	35.208	234.438^{b}	16.019	3231.191^{bcde}	25.492	3022.814^{bcde}	42.045
13	813.812^{a}	102.866	470.999^{a}	43.505	3852.410^{bcde}	80.536	3043.216^{abcd}	62.460
14	396.469^{b}	63.167	202.598^{b}	29.027	3501.832^{bcde}	52.252	1986.357^{bcde}	389.191
15	301.656^{b}	99.957	222.174^{b}	34.998	3206.072^{bcde}	79.038	2134.473^{bcde}	54.040
16	338.803^{b}	46.453	286.090^{b}	68.316	3667.519^{bcde}	26.553	2663.374^{bcde}	32.075
17	427.838^{ab}	55.012	291.161^{ab}	38.091	3266.569^{cde}	73.346	1296.250^{cde}	95.120
18	449.065^{ab}	95.087	289.274^{ab}	33.789	3843.112^{bcde}	74.526	2291.315^{bcde}	112.408
19	314.746^{b}	50.460	219.697^{b}	57.447	2664.317^{de}	292.713	1443.776^{de}	65.841
20	398.002^{ab}	60.747	288.567^{ab}	34.139	3165.034^{bcde}	22.999	3519.639^{bcde}	36.659
21	369.464^{b}	39.530	233.849^{b}	23.829	5636.895^{abcd}	142.978	5601.517^{abcd}	124.243
22	264.627^{b}	73.081	245.287^{b}	44.385	5896.333^{ab}	691.758	6812.624^{ab}	203.426
23	306.963^{b}	84.978	290.571^{b}	31.882	5534.534^{abcd}	118.591	5612.130^{abcd}	55.525
24	325.242^{b}	54.291	231.490^{b}	20.169	6571.110^{a}	120.028	7589.760^{a}	76.887
25	313.213^{b}	81.461	285.265^{b}	59.099	6845.643^{abc}	135.132	5209.293^{abc}	85.102
26	220.995^{b}	63.479	201.895^{b}	39.421	731.971^{e}	48.117	1058.628^{e}	453.342

2024, 21(3): 0867-0893
https://dx.doi.org/10.21123/bsj.2023.8382
P-ISSN: 2078-8665 - E-ISSN: 2411-7986
Baghdad Science Journal

Table 5. Standard deviation (SD) of (Ni and Cu) and Means (mg kg^{-1}, Dry Weight) of study soil samples the same row followed by different letters are significantly different at $p < 0.05$ during summer.

Parameters	Ni				Cu			
Depth	**0-5 cm**		**5-30 cm**		**0-5 cm**		**5-30 cm**	
Sites	**Mean**	**SD**	**Mean**	**SD**	**Mean**	**SD**	**Mean**	**SD**
1	176.890[c]	15.420	163.918[c]	8.903	130.899[ab]	27.631	130.899[ab]	9.360
2	247.646[abc]	35.378	117.927[abc]	5.404	166.277[ab]	26.709	90.804[ab]	11.372
3	202.834[abc]	35.613	194.579[abc]	26.709	163.918[ab]	42.502	127.361[ab]	38.915
4	212.268[abc]	35.378	279.486[abc]	24.764	283.024[a]	35.378	261.797[a]	35.378
5	141.512[abc]	35.378	274.769[abc]	19.484	91.983[b]	7.075	100.238[b]	7.364
6	266.514[abc]	42.649	189.862[abc]	37.828	136.795[ab]	23.018	90.804[ab]	7.364
7	201.655[abc]	19.697	198.117[abc]	10.613	117.927[ab]	20.425	143.871[ab]	20.116
8	242.929[abc]	15.952	188.683[abc]	40.851	163.918[ab]	20.729	145.050[ab]	12.755
9	283.024[abc]	40.181	143.871[abc]	20.116	182.786[ab]	19.484	115.568[ab]	31.905
10	221.702[abc]	35.613	201.655[abc]	50.156	166.277[ab]	37.273	106.134[ab]	35.378
11	261.797[abc]	25.511	215.806[abc]	30.226	188.683[ab]	54.040	121.464[ab]	16.718
12	241.750[abc]	32.871	188.683[abc]	54.040	169.814[ab]	21.226	172.173[ab]	73.645
13	198.117[abc]	34.117	265.335[abc]	72.243	141.512[ab]	70.756	173.352[ab]	39.868
14	253.542[abc]	33.626	295.996[abc]	35.613	193.400[ab]	78.259	200.475[ab]	89.032
15	295.637[abc]	34.117	241.750[abc]	14.297	121.464[ab]	30.088	107.313[ab]	18.154
16	280.665[abc]	58.382	154.484[abc]	42.796	93.162[b]	26.077	95.521[b]	26.709
17	212.268[abc]	35.378	212.268[abc]	44.328	176.890[ab]	65.520	130.899[ab]	38.267
18	260.618[abc]	58.809	161.560[abc]	41.459	180.428[ab]	59.092	200.475[ab]	73.645
19	166.277[abc]	34.843	188.683[abc]	54.040	107.903[a b]	26.057	156.842[ab]	73.560
20	235.853[abc]	46.172	224.061[abc]	31.905	166.277[ab]	42.893	245.287[ab]	77.938
21	528.311[abc]	142.978	296.232[abc]	124.243	156.842[ab]	24.081	176.890[ab]	35.378
22	529.491[abc]	691.758	366.752[abc]	203.426	172.173[ab]	60.177	191.041[ab]	53.067
23	577.841[ab]	118.591	346.704[ab]	55.525	106.134[ab]	35.378	115.568[ab]	56.641
24	640.340[a]	120.028	314.864[a]	76.887	156.842[ab]	27.479	141.512[ab]	35.378
25	412.743[abc]	135.132	235.853[abc]	85.102	232.316[ab]	47.771	198.117[ab]	85.860
26	129.719[c]	48.117	182.786[c]	453.342	141.512[ab]	44.328	174.531[ab]	61.919

Table 6. Standard deviation (SD) of (Cr and Hg) and Means (mg kg^{-1}, Dry Weight) of study soil samples the same row followed by different letters are significantly different at $p < 0.05$ during summer.

Parameters	Cr				Hg			
Depth	**0-5 cm**		**5-30 cm**		**0-5 cm**		**5-30 cm**	
Sites	**Mean**	**SD**	**Mean**	**SD**	**Mean**	**SD**	**Mean**	**SD**
1	61.322^{d}	5.404	106.134^{d}	35.378	0.213^{c}	0.026	0.213^{c}	0.026
2	114.389^{cd}	26.077	73.115^{cd}	7.364	0.319^{bc}	0.026	0.213^{bc}	0.026
3	101.417^{cd}	35.436	117.927^{cd}	20.425	0.727^{bc}	0.155	0.505^{bc}	0.026
4	185.145^{cd}	37.160	136.795^{cd}	20.729	0.319^{c}	0.026	0.186^{c}	0.026
5	81.369^{cd}	21.519	97.879^{cd}	18.154	1.011^{bc}	0.026	0.186^{bc}	0.026
6	115.568^{cd}	31.905	67.218^{cd}	3.537	0.399^{bc}	0.026	0.390^{bc}	0.081
7	93.162^{cd}	5.404	139.153^{cd}	12.424	0.364^{bc}	0.040	0.355^{bc}	0.066
8	141.512^{cd}	35.378	146.229^{cd}	5.404	0.709^{bc}	0.406	0.532^{bc}	0.266
9	175.711^{cd}	41.003	147.408^{cd}	35.436	0.186^{bc}	0.026	0.381^{bc}	0.066
10	201.655^{cd}	28.958	206.372^{cd}	46.172	0.168^{c}	0.040	0.293^{c}	0.026
11	293.637^{abcd}	31.840	412.743^{abcd}	30.008	0.160^{c}	0.053	0.186^{c}	0.026
12	306.609^{abcd}	54.040	224.061^{abcd}	54.040	0.177^{bc}	0.040	0.426^{bc}	0.095
13	232.316^{abcd}	46.172	306.609^{abcd}	54.040	0.195^{c}	0.040	0.160^{c}	0.053
14	391.517^{abc}	54.845	413.923^{abc}	30.226	0.177^{c}	0.066	0.133^{c}	0.053
15	353.780^{abcd}	35.378	336.091^{abcd}	27.631	0.133^{c}	0.070	0.168^{c}	0.040
16	353.780^{abcd}	70.756	377.365^{abcd}	54.040	0.399^{bc}	0.079	0.168^{bc}	0.055
17	566.048^{a}	106.134	518.788^{a}	108.081	0.168^{bc}	0.066	0.426^{bc}	0.095
18	365.573^{abcd}	54.040	353.780^{abcd}	54.921	1.286^{a}	0.998	1.179^{a}	0.744
19	283.024^{abcd}	35.378	448.121^{abcd}	142.978	0.434^{ab}	0.040	1.232^{ab}	0.199
20	554.255^{ab}	73.645	507.085^{ab}	89.032	0.408^{bc}	0.093	0.381^{bc}	0.085
21	200.475^{cd}	54.040	247.646^{cd}	93.601	0.559^{bc}	0.053	0.160^{bc}	0.053
22	212.268^{bcd}	70.756	259.439^{bcd}	73.645	0.390^{bc}	0.066	0.399^{bc}	0.095
23	341.987^{abcd}	54.040	377.719^{abcd}	61.374	0.364^{bc}	0.055	0.479^{bc}	0.095
24	345.525^{abcd}	82.993	283.024^{abcd}	35.378	1.011^{bc}	0.106	0.372^{bc}	0.053
25	294.817^{abcd}	72.876	331.374^{abcd}	42.502	0.364^{bc}	0.081	0.381^{bc}	0.085
26	332.553^{abcd}	59.092	382.082^{abcd}	37.273	0.505^{bc}	0.053	0.168^{bc}	0.066

Table 7. Standard deviation (SD) of (Zn and Cd) and Means ($mg\ kg^{-1}$, Dry Weight) of study soil samples the same row followed by different letters are significantly different at $p < 0.05$ during winter.

Parameters	**Zn**				**Cd**			
Depth	**0-5 cm**		**5-30 cm**		**0-5 cm**		**5-30 cm**	
Sites	**Mean**	**SD**	**Mean**	**SD**	**Mean**	**SD**	**Mean**	**SD**
1	14.930^{a}	0.035	14.788^{a}	0.035	1.769^{ab}	0.353	2.005^{ab}	0.073
2	54.411^{abcd}	0.035	32.654^{abcd}	0.035	1.097^{b}	0.953	1.250^{b}	0.124
3	117.561^{bcd}	0.035	106.665^{bcd}	0.035	1.769^{b}	1.061	1.238^{b}	0.106
4	17.618^{bcd}	0.035	21.463^{bcd}	0.540	1.061^{ab}	0.093	0.778^{ab}	0.106
5	14.151^{cd}	0.353	17.088^{cd}	0.035	0.653^{ab}	0.010	0.645^{ab}	0.017
6	14.611^{abcd}	0.035	45.708^{abcd}	0.035	0.445^{ab}	0.010	1.545^{ab}	0.159
7	9.800^{bcd}	0.035	9.021^{bcd}	0.035	0.814^{ab}	0.141	1.144^{ab}	0.181
8	12.913^{abcd}	0.196	13.161^{abcd}	0.035	1.309^{ab}	0.162	1.309^{ab}	0.162
9	20.696^{abcd}	0.035	13.267^{abcd}	0.035	4.198^{b}	0.089	1.191^{b}	0.102
10	26.357^{abcd}	0.035	39.906^{abcd}	0.035	1.344^{b}	0.106	2.382^{b}	0.142
11	138.788^{ab}	0.035	113.740^{ab}	0.035	9.611^{ab}	0.108	4.894^{ab}	0.248
12	76.735^{ab}	0.035	68.583^{ab}	0.035	2.547^{ab}	0.127	1.580^{ab}	0.142
13	51.157^{abcd}	0.035	130.616^{abcd}	0.035	1.875^{ab}	0.093	5.425^{ab}	0.890
14	20.696^{abcd}	0.035	16.345^{abcd}	0.035	2.005^{b}	0.736	2.123^{b}	0.936
15	42.347^{abcd}	0.035	30.496^{abcd}	0.035	1.580^{ab}	0.142	1.696^{ab}	0.124
16	25.012^{abcd}	0.035	21.757^{abcd}	0.035	1.769^{ab}	1.061	1.981^{ab}	0.106
17	15.767^{abc}	0.054	17.595^{abc}	0.073	1.557^{ab}	0.106	1.415^{ab}	0.353
18	15.460^{abcd}	0.035	13.915^{abcd}	0.736	1.557^{ab}	0.106	1.580^{ab}	0.142
19	18.467^{abcd}	0.035	10.755^{abcd}	0.070	2.123^{ab}	0.936	1.450^{ab}	0.106
20	29.517^{abcd}	0.124	51.841^{abcd}	0.124	1.167^{ab}	0.162	1.486^{ab}	0.187
21	16.781^{abcd}	0.124	14.033^{abcd}	0.890	1.344^{a}	0.280	1.498^{a}	0.201
22	15.413^{abcd}	0.147	14.788^{abcd}	0.106	2.005^{ab}	0.736	1.321^{ab}	0.178
23	28.939^{abcd}	0.196	21.769^{abcd}	0.124	2.241^{ab}	0.181	2.229^{ab}	0.162
24	26.097^{abcd}	0.194	33.692^{abcd}	0.235	1.851^{ab}	0.124	2.217^{ab}	0.142
25	14.422^{abcd}	0.159	13.927^{abcd}	0.159	1.710^{ab}	0.142	1.368^{ab}	0.142
26	12.312^{d}	0.106	15.496^{d}	0.127	1.109^{ab}	0.159	1.344^{ab}	0.141

2024, 21(3): 0867-0893
https://dx.doi.org/10.21123/bsj.2023.8382
P-ISSN: 2078-8665 - E-ISSN: 2411-7986
Baghdad Science Journal

Table 8. Standard deviation (SD) of (Pb and Mn) and Means (mg kg^{-1}, Dry Weight) of study soil samples the same row followed by different letters are significantly different at $p < 0.05$ during winter.

Parameters	Pb				Mn			
Depth	**0-5 cm**		**5-30 cm**		**0-5 cm**		**5-30 cm**	
Sites	**Mean**	**SD**	**Mean**	**SD**	**Mean**	**SD**	**Mean**	**SD**
1	20.260^{ab}	0.167	17.677^{ab}	0.054	73.822^{e}	1.242	56.015^{e}	1.242
2	17.713^{b}	0.073	15.142^{b}	0.196	73.468^{bcde}	1.815	112.266^{bcde}	0.540
3	20.213^{b}	0.089	20.213^{b}	0.124	85.851^{bcde}	3.190	93.752^{bcde}	3.891
4	17.677^{b}	0.089	20.236^{b}	0.127	84.671^{bcde}	11.256	89.388^{bcde}	8.500
5	22.772^{b}	0.178	20.201^{b}	0.106	81.134^{de}	7.688	70.756^{de}	3.537
6	20.272^{b}	0.093	17.665^{b}	0.073	75.119^{bcde}	16.382	88.445^{bcde}	7.075
7	15.142^{ab}	0.196	12.418^{ab}	0.308	80.898^{e}	7.833	54.246^{e}	12.424
8	20.213^{ab}	0.159	17.654^{ab}	0.162	74.058^{e}	1.948	72.053^{e}	8.725
9	45.473^{ab}	0.248	17.654^{ab}	0.127	95.521^{cde}	5.845	85.851^{cde}	13.351
10	17.029^{b}	1.205	20.224^{b}	0.108	86.440^{bcde}	3.976	134.554^{bcde}	31.750
11	73.303^{ab}	0.106	47.890^{ab}	0.147	129.130^{bcde}	42.811	148.588^{bcde}	62.448
12	37.961^{b}	0.162	43.114^{b}	0.178	167.810^{bcde}	17.519	145.757^{bcde}	20.905
13	27.807^{a}	0.283	48.987^{a}	1.457	83.492^{bcde}	20.298	103.893^{bcde}	28.772
14	20.378^{b}	0.408	17.654^{b}	0.127	146.111^{bcde}	26.208	175.829^{bcde}	31.210
15	23.479^{b}	3.420	25.342^{b}	0.207	174.531^{bcde}	24.311	120.167^{bcde}	36.976
16	20.472^{b}	0.568	23.467^{b}	3.428	67.572^{bcde}	5.353	74.530^{bcde}	7.157
17	17.642^{ab}	0.113	24.682^{ab}	2.147	108.021^{cde}	23.809	84.907^{cde}	10.332
18	20.071^{ab}	0.791	20.071^{ab}	1.176	95.403^{bcde}	8.023	88.799^{bcde}	5.845
19	17.595^{b}	0.328	15.165^{b}	0.265	91.629^{de}	12.106	86.204^{de}	13.318
20	15.590^{ab}	0.445	17.724^{ab}	0.196	80.780^{bcde}	3.543	74.766^{bcde}	13.798
21	21.215^{b}	0.089	19.175^{b}	0.649	105.426^{abcd}	6.288	91.983^{abcd}	3.537
22	41.274^{b}	5.404	20.956^{b}	0.500	61.794^{ab}	8.825	62.147^{ab}	9.729
23	21.015^{b}	0.495	19.493^{b}	0.782	98.115^{abcd}	14.510	62.501^{abcd}	8.493
24	18.998^{b}	0.348	28.067^{b}	0.471	60.143^{a}	9.360	79.600^{a}	15.626
25	16.333^{b}	0.194	16.345^{b}	0.984	77.596^{abc}	4.130	79.011^{abc}	14.729
26	16.345^{b}	0.984	13.927^{b}	0.482	64.034^{e}	12.945	1.014^{e}	19.972

Table 9. Standard deviation (SD) of (Ni and Cu) and Means (mg kg^{-1}, Dry Weight) of study soil samples the same row followed by different letters are significantly different at $p < 0.05$ during winter.

Parameters	Ni				Cu			
Depth	**0-5 cm**		**5-30 cm**		**0-5 cm**		**5-30 cm**	
Sites	**Mean**	**SD**	**Mean**	**SD**	**Mean**	**SD**	**Mean**	**SD**
1	1.934^{c}	0.354	1.262^{c}	0.305	6.451^{ab}	0.475	4.823^{ab}	0.235
2	1.285^{abc}	0.300	1.580^{abc}	0.294	10.578^{ab}	1.482	8.538^{ab}	0.742
3	1.002^{abc}	0.194	1.061^{abc}	0.353	8.219^{ab}	0.950	6.462^{ab}	0.488
4	0.896^{abc}	0.073	1.297^{abc}	0.250	5.790^{a}	0.425	8.373^{a}	0.250
5	1.002^{abc}	0.213	1.073^{abc}	0.113	8.302^{b}	0.368	6.557^{b}	0.363
6	0.825^{abc}	0.142	2.005^{abc}	0.736	11.427^{ab}	0.393	12.076^{ab}	0.108
7	1.050^{abc}	0.074	1.262^{abc}	0.319	6.627^{ab}	0.108	4.528^{ab}	0.127
8	1.144^{abc}	0.394	1.238^{abc}	0.314	8.078^{ab}	0.108	6.321^{ab}	0.456
9	1.356^{abc}	0.488	1.415^{abc}	0.936	11.321^{ab}	0.231	4.894^{ab}	0.124
10	1.403^{abc}	0.178	2.193^{abc}	0.775	8.255^{ab}	0.201	12.146^{ab}	1.080
11	1.816^{abc}	0.559	1.698^{abc}	0.942	101.476^{ab}	0.768	65.791^{ab}	5.741
12	2.123^{abc}	0.707	1.651^{abc}	0.250	26.769^{ab}	2.484	23.585^{ab}	5.404
13	1.604^{abc}	0.230	1.380^{abc}	0.141	20.319^{ab}	0.283	54.246^{ab}	13.848
14	1.557^{abc}	0.582	2.241^{abc}	1.815	14.151^{ab}	2.209	22.182^{ab}	0.579
15	8.373^{abc}	9.375	1.580^{abc}	0.983	29.446^{ab}	0.334	6.156^{ab}	0.348
16	1.792^{abc}	0.442	1.215^{abc}	0.113	11.793^{b}	5.404	5.106^{b}	0.978
17	0.979^{abc}	0.108	1.279^{abc}	1.080	12.241^{ab}	0.951	8.090^{ab}	0.167
18	1.279^{abc}	0.167	0.979^{abc}	0.159	11.793^{ab}	11.372	16.510^{ab}	7.364
19	1.368^{abc}	0.124	1.887^{abc}	0.736	12.029^{ab}	6.137	7.913^{ab}	0.343
20	1.568^{abc}	0.378	1.014^{abc}	0.124	8.491^{ab}	1.148	9.517^{ab}	0.765
21	0.896^{abc}	0.230	2.123^{abc}	1.061	9.493^{ab}	0.216	6.014^{ab}	0.267
22	1.215^{abc}	0.178	1.002^{abc}	0.265	9.151^{ab}	1.087	8.668^{ab}	0.963
23	1.533^{ab}	1.137	1.533^{ab}	0.736	12.429^{ab}	1.133	12.972^{ab}	5.404
24	0.991^{a}	0.106	1.191^{a}	0.147	8.668^{ab}	0.963	8.396^{ab}	0.283
25	0.849^{abc}	0.093	1.533^{abc}	0.890	15.330^{ab}	11.372	10.024^{ab}	0.618
26	1.568^{c}	12.945	0.240^{c}	19.972	0.743^{ab}	0.540	5.307^{ab}	0.353

2024, 21(3): 0867-0893
https://dx.doi.org/10.21123/bsj.2023.8382
P-ISSN: 2078-8665 - E-ISSN: 2411-7986
Baghdad Science Journal

Table 10. Standard deviation (SD) of (Cr and Hg) and Means (mg kg^{-1}, Dry Weight) of study soil samples the same row followed by different letters are significantly different at $p < 0.05$ during winter.

Parameters	**Cr**				**Hg**			
Depth	**0-5 cm**		**5-30 cm**		**0-5 cm**		**5-30 cm**	
Sites	**Mean**	**SD**	**Mean**	**SD**	**Mean**	**SD**	**Mean**	**SD**
1	7.984^{d}	0.089	7.866^{d}	0.248	0.013^{c}	0.002	0.038^{c}	0.008
2	11.911^{cd}	0.089	9.399^{cd}	0.425	0.010^{bc}	0.006	0.016^{bc}	0.007
3	9.941^{cd}	0.556	9.658^{cd}	0.984	0.012^{bc}	0.006	0.012^{bc}	0.005
4	8.184^{cd}	0.368	8.043^{cd}	0.207	0.011^{c}	0.004	0.012^{c}	0.004
5	9.764^{cd}	0.289	7.571^{cd}	0.141	0.016^{bc}	0.007	0.008^{bc}	0.007
6	12.547^{cd}	0.413	7.618^{cd}	0.181	0.011^{bc}	0.007	0.015^{bc}	0.005
7	10.130^{cd}	0.371	7.783^{cd}	0.231	0.013^{bc}	0.007	0.013^{bc}	0.007
8	10.106^{cd}	0.371	12.547^{cd}	0.309	0.017^{bc}	0.008	0.020^{bc}	0.005
9	8.078^{cd}	0.454	9.788^{cd}	0.461	0.012^{bc}	0.005	0.012^{bc}	0.006
10	7.936^{cd}	0.391	5.814^{cd}	0.397	0.012^{c}	0.005	0.013^{c}	0.005
11	8.373^{abcd}	0.609	9.741^{abcd}	0.363	0.012^{c}	0.004	0.011^{c}	0.009
12	5.672^{abcd}	0.568	5.849^{abcd}	0.410	0.008^{bc}	0.007	0.009^{bc}	0.004
13	5.908^{abcd}	0.389	7.889^{abcd}	0.176	0.008^{c}	0.002	0.009^{c}	0.004
14	7.913^{abc}	0.354	8.007^{abc}	0.334	0.012^{c}	0.004	0.010^{c}	0.005
15	5.885^{abcd}	0.425	7.748^{abcd}	0.141	0.008^{c}	0.002	0.010^{c}	0.005
16	5.814^{abcd}	0.328	8.880^{abcd}	1.158	0.012^{bc}	0.005	0.008^{bc}	0.002
17	9.811^{a}	0.743	8.031^{a}	0.579	0.011^{bc}	0.004	0.008^{bc}	0.005
18	9.010^{abcd}	1.373	9.057^{abcd}	1.287	0.010^{a}	0.003	0.010^{a}	0.006
19	6.014^{abcd}	0.707	7.311^{abcd}	0.736	0.007^{ab}	0.004	0.012^{ab}	0.004
20	5.307^{ab}	1.061	8.373^{ab}	1.429	0.006^{bc}	0.004	0.009^{bc}	0.005
21	12.029^{cd}	6.288	4.717^{cd}	0.736	0.012^{bc}	0.005	0.013^{bc}	0.004
22	6.368^{bcd}	1.061	9.198^{bcd}	5.845	0.036^{bc}	0.004	0.012^{bc}	0.001
23	6.014^{abcd}	0.707	6.486^{abcd}	1.429	0.012^{bc}	0.004	0.015	0.004
24	9.552^{abcd}	2.895	6.132^{abcd}	0.736	0.012^{bc}	0.004	0.010	0.004
25	7.076^{abcd}	2.670	9.434^{abcd}	1.948	0.014^{bc}	0.006	0.013	0.002
26	10.260^{abcd}	1.061	6.368^{abcd}	1.542	0.005^{bc}	0.002	0.006	0.004

2024, 21(3): 0867-0893
https://dx.doi.org/10.21123/bsj.2023.8382
P-ISSN: 2078-8665 - E-ISSN: 2411-7986
Baghdad Science Journal

Assessment of Contamination Risk Using Geoaccumulation Index:

In this investigation, soil contamination was evaluated using I-geo. In the various soil layers, the I-geo results showed widespread contamination by Zn, Cd, Pb, Mn, Ni, Cu, Cr, and Hg. In summer, I-geo (Zn) ranged from -1.700 to 3.560, indicating that the concentration of Zn in landfill soils ranges from uncontaminated to strongly contaminated ,Tables 11 and 12 [43], I-geo (Cd) values varied from 5.045 to 8.175 are classified as extremely contaminated; I-geo (Pb) values varied from 2.318 to 4.329 are classified as moderately/strongly contaminated to strongly/extremely contaminated; I-geo (Mn) values varied from 0 to 3.374 are classified as uncontaminated to strongly contaminated, and I-geo (Ni) values ranging from 1.439 to 3.880, I-geo (Cu) values between 0.638 and 2.278 are classified as Uncontaminated/moderately contaminated to Moderately/strongly contaminated. I-geo (Cr) ranged from -0.541 and 2.665 are categorized as uncontaminated to Moderately/strongly contaminated Tables. 11 and 12.

Table 11. Geoaccumulation index (I-geo) for (Zn, Cd, Pb and Mn) during summer.

Parameters	**Zn**		**Cd**		**Pb**		**Mn**	
Depth	**0-5 cm**	**5-30 cm**	**0-5 cm**	**5-30 cm**	**0-5 cm**	**5-30 cm**	**0-5 cm**	**5-30 cm**
Background	**70**		**0.41**		**27**		**488**	
1	0.714	3.560	8.168	5.431	4.070	3.057	0.855	1.450
2	1.337	1.131	6.369	6.290	3.068	2.342	1.227	2.755
3	0.266	-0.154	5.035	6.372	2.754	2.533	2.190	1.226
4	1.337	0.932	7.357	7.239	2.922	2.779	2.040	2.277
5	0.546	0.491	6.563	6.509	2.812	2.826	1.221	1.606
6	2.515	0.694	6.536	6.369	2.905	2.978	2.148	1.616
7	0.790	0.905	7.705	5.572	3.192	3.001	0.299	1.448
8	1.933	0.698	6.536	7.667	3.599	3.422	2.263	1.976
9	1.860	1.047	6.653	5.640	3.565	2.815	2.281	0.827
10	2.752	0.781	6.125	6.478	2.832	3.145	2.110	1.999
11	1.799	2.663	6.236	7.238	2.835	3.257	2.415	1.770
12	2.968	1.547	6.741	6.728	2.829	2.533	2.142	2.046
13	1.380	1.503	6.681	6.754	4.329	3.540	2.396	2.056
14	1.872	1.178	5.827	6.506	3.291	2.323	2.258	1.440
15	1.973	0.101	6.662	6.846	2.897	2.456	2.131	1.544
16	2.798	0.909	6.574	6.258	3.064	2.820	2.325	1.863
17	2.873	1.405	6.097	7.583	3.401	2.846	2.158	0.824
18	2.574	0.565	7.405	6.955	3.471	2.836	2.392	1.646
19	1.730	0.404	7.252	7.940	2.958	2.440	1.864	0.980
20	1.022	1.073	8.175	7.631	3.297	2.833	2.112	2.266
21	2.160	1.314	7.202	6.710	3.189	2.530	2.945	2.936
22	2.734	1.302	8.118	6.950	2.708	2.598	3.010	3.218
23	2.573	1.969	6.957	7.569	2.922	2.843	2.919	2.939
24	2.720	1.485	7.698	7.330	3.006	2.515	3.166	3.374
25	2.643	1.332	6.856	5.879	2.951	2.816	3.225	2.831
26	-1.700	-0.543	7.153	6.836	2.448	2.318	0.000	0.532

2024, 21(3): 0867-0893
https://dx.doi.org/10.21123/bsj.2023.8382
P-ISSN: 2078-8665 - E-ISSN: 2411-7986

Table 12. Geoaccumulation index (I-geo) for (Ni, Cu, Cr and Hg) during summer.

Parameters	**Ni**		**Cu**		**Cr**		**Hg**	
Depth	**0-5 cm**	**5-30 cm**	**0-5 cm**	**5-30 cm**	**0-5 cm**	**5-30 cm**	**0-5 cm**	**5-30 cm**
Background	**29**		**38.9**		**59.5**		**0.50**	
1	2.024	1.914	1.166	1.166	-0.541	0.250	-1.816	-1.816
2	2.509	1.439	1.511	0.638	0.358	-0.288	-1.233	-1.816
3	2.221	2.161	1.490	1.126	0.184	0.402	-0.045	-0.571
4	2.287	2.684	2.278	2.166	1.053	0.616	-1.233	-2.012
5	1.702	2.659	0.657	0.781	-0.133	0.133	0.431	-2.012
6	2.615	2.126	1.229	0.638	0.373	-0.409	-0.911	-0.943
7	2.213	2.187	1.015	1.302	0.062	0.641	-1.043	-1.079
8	2.481	2.117	1.490	1.314	0.665	0.712	-0.081	-0.495
9	2.702	1.726	1.647	0.986	0.977	0.724	-2.012	-0.977
10	2.350	2.213	1.511	0.863	1.176	1.209	-2.158	-1.356
11	2.589	2.311	1.693	1.058	1.718	2.209	-2.229	-2.012
12	2.474	2.117	1.541	1.561	1.780	1.328	-2.083	-0.816
13	2.187	2.609	1.278	1.571	1.380	1.780	-1.943	-2.229
14	2.543	2.766	1.729	1.781	2.133	2.213	-2.083	-2.495
15	2.765	2.474	1.058	0.879	1.987	1.913	-2.495	-2.158
16	2.690	1.828	0.675	0.711	1.987	2.080	-0.911	-2.158
17	2.287	2.287	1.600	1.166	2.665	2.539	-2.158	-0.816
18	2.583	1.893	1.629	1.781	2.034	1.987	0.778	0.653
19	1.935	2.117	0.887	1.427	1.665	2.328	-0.789	0.716
20	2.439	2.365	1.511	2.072	2.635	2.506	-0.878	-0.977
21	3.602	2.768	1.427	1.600	1.167	1.472	-0.424	-2.229
22	3.606	3.076	1.561	1.711	1.250	1.539	-0.943	-0.911
23	3.732	2.995	0.863	0.986	1.938	2.081	-1.043	-0.647
24	3.880	2.856	1.427	1.278	1.953	1.665	0.431	-1.012
25	3.246	2.439	1.993	1.764	1.724	1.893	-1.043	-0.977
26	1.576	2.071	1.278	1.581	1.898	2.098	-0.571	-2.158

In contrast, during winter, I-geo values for all heavy metals were classified as uncontaminated, with the notable exception of I-geo (Cd), which varied from -0.467 to 3.966 and was classified as uncontaminated to strong, and I-geo (Ni), which ranged from -5.720 to 2.015 and was classified as

2024, 21(3): 0867-0893
https://dx.doi.org/10.21123/bsj.2023.8382
P-ISSN: 2078-8665 - E-ISSN: 2411-7986
Baghdad Science Journal

uncontaminated to moderately/heavily contaminated, Tables 13 and 14. Lower levels of heavy metals in winter due to the leaching of heavy metals by precipitation.

Table 13. Geoaccumulation index (I-geo) for (Zn, Cd, Pb and Mn) during winter.

Parameters	**Zn**		**Cd**		**Pb**		**Mn**	
Depth	**0-5 cm**	**5-30 cm**	**0-5 cm**	**5-30 cm**	**0-5 cm**	**5-30 cm**	**0-5 cm**	**5-30 cm**
Background	**70**		**0.41**		**27**		**488**	
1	-2.814	-2.828	1.524	1.705	-0.999	-1.196	-3.310	-3.708
2	-0.948	-1.685	0.835	1.023	-1.193	-1.419	-3.317	-2.705
3	0.163	0.023	1.524	1.009	-1.003	-1.003	-3.092	-2.965
4	-2.575	-2.290	0.787	0.339	-1.196	-1.001	-3.112	-3.034
5	-2.891	-2.619	0.086	0.069	-0.831	-1.003	-3.173	-3.371
6	-2.845	-1.200	-0.467	1.329	-0.998	-1.197	-3.285	-3.049
7	-3.421	-3.541	0.404	0.895	-1.419	-1.705	-3.178	-3.754
8	-3.023	-2.996	1.090	1.090	-1.003	-1.198	-3.305	-3.345
9	-2.343	-2.984	2.771	0.954	0.167	-1.198	-2.938	-3.092
10	-1.994	-1.396	1.128	1.954	-1.250	-1.002	-3.082	-2.444
11	0.402	0.115	3.966	2.992	0.856	0.242	-2.503	-2.301
12	-0.452	-0.614	2.050	1.361	-0.093	0.090	-2.125	-2.328
13	-1.037	0.315	1.608	3.141	-0.542	0.274	-3.132	-2.817
14	-2.343	-2.683	1.705	1.787	-0.991	-1.198	-2.325	-2.058
15	-1.310	-1.784	1.361	1.463	-0.787	-0.676	-2.068	-2.607
16	-2.070	-2.271	1.524	1.688	-0.984	-0.787	-3.437	-3.296
17	-2.735	-2.577	1.340	1.202	-1.199	-0.714	-2.761	-3.108
18	-2.764	-2.916	1.340	1.361	-1.013	-1.013	-2.940	-3.043
19	-2.507	-3.287	1.787	1.237	-1.203	-1.417	-2.998	-3.086
20	-1.831	-1.018	0.924	1.273	-1.377	-1.192	-3.180	-3.291
21	-2.645	-2.903	1.128	1.284	-0.933	-1.079	-2.796	-2.992
22	-2.768	-2.828	1.705	1.103	0.027	-0.951	-3.566	-3.558
23	-1.859	-2.270	1.865	1.858	-0.947	-1.055	-2.899	-3.550
24	-2.008	-1.640	1.590	1.850	-1.092	-0.529	-3.605	-3.201
25	-2.864	-2.914	1.475	1.153	-1.310	-1.309	-3.238	-3.212
26	-3.092	-2.760	0.851	1.128	-1.309	-1.540	-3.515	-9.496

2024, 21(3): 0867-0893
https://dx.doi.org/10.21123/bsj.2023.8382
P-ISSN: 2078-8665 - E-ISSN: 2411-7986
Baghdad Science Journal

Table 14. Geoaccumulation index (I-geo) for (Ni, Cu, Cr and Hg) during winter.

Parameters	**Ni**		**Cu**		**Cr**		**Hg**	
Depth	**0-5 cm**	**5-30 cm**	**0-5 cm**	**5-30 cm**	**0-5 cm**	**5-30 cm**	**0-5 cm**	**5-30 cm**
Background	**29**		**38.9**		**59.5**		**0.50**	
1	-4.491	0.365	-3.177	-3.597	-3.483	-3.504	-5.850	-4.303
2	-5.081	1.368	-2.464	-2.773	-2.906	-3.247	-6.229	-5.551
3	-5.440	1.108	-2.828	-3.175	-3.166	-3.208	-5.966	-5.966
4	-5.601	1.039	-3.333	-2.801	-3.447	-3.472	-6.091	-5.966
5	-5.440	0.702	-2.813	-3.154	-3.192	-3.559	-5.551	-6.551
6	-5.720	1.024	-2.352	-2.273	-2.831	-3.550	-6.091	-5.644
7	-5.373	0.319	-3.138	-3.688	-3.139	-3.519	-5.850	-5.850
8	-5.249	0.728	-2.853	-3.207	-3.143	-2.831	-5.463	-5.229
9	-5.004	0.981	-2.366	-3.576	-3.466	-3.189	-5.966	-5.966
10	-4.954	1.629	-2.821	-2.264	-3.491	-3.940	-5.966	-5.850
11	-4.582	1.772	0.798	0.173	-3.414	-3.196	-5.966	-6.091
12	-4.357	1.744	-1.124	-1.307	-3.976	-3.932	-6.551	-6.381
13	-4.761	1.256	-1.522	-0.105	-3.917	-3.500	-6.551	-6.381
14	-4.804	2.015	-2.044	-1.395	-3.496	-3.479	-5.966	-6.229
15	-2.377	1.466	-0.987	-3.245	-3.923	-3.526	-6.551	-6.229
16	-4.601	0.777	-2.307	-3.514	-3.940	-3.329	-5.966	-6.551
17	-5.474	0.965	-2.253	-2.851	-3.185	-3.474	-6.091	-6.551
18	-5.088	1.030	-2.307	-1.821	-3.308	-3.301	-6.229	-6.229
19	-4.991	0.987	-2.278	-2.882	-3.891	-3.610	-6.743	-5.966
20	-4.794	0.781	-2.781	-2.616	-4.072	-3.414	-6.966	-6.381
21	-5.601	1.080	-2.620	-3.278	-2.891	-4.242	-5.966	-5.850
22	-5.162	0.515	-2.673	-2.751	-3.809	-3.278	-4.381	-5.966
23	-4.827	0.523	-2.231	-2.169	-3.891	-3.782	-5.966	-5.644
24	-5.456	0.872	-2.751	-2.797	-3.224	-3.863	-5.966	-6.229
25	-5.679	0.861	-1.928	-2.541	-3.657	-3.242	-5.743	-5.850
26	-4.794	-5.423	-6.295	-3.459	-3.121	-3.809	-7.229	-6.966

Figs. 5–7 depict the spatial distributions of I-geo during summer for heavy metals in the study area. The maps of the Cd distributions are entirely colored differently, showing that the soil layers of study sites were extremely contaminated with Cd. Furthermore, increasing concentrations of Pb in soil

2024, 21(3): 0867-0893
https://dx.doi.org/10.21123/bsj.2023.8382
P-ISSN: 2078-8665 - E-ISSN: 2411-7986
Baghdad Science Journal

layers were noted with increasing concentrations towards the middle portions of the study area, which might be related to the proximity to significant waste accumulations that may encompass batteries. Most of the work area is orange on the Ni maps, which means that a large part of the area being looked into was moderate to strongly contaminated with Ni.

Consequently, the spatial distribution of I- geo heavy metals throughout winter was categorized as uncontaminated to moderately/strongly contaminated, Figs. 8–10. The Cd distribution maps are entirely yellow, indicating that the study region was moderately contaminated with Cd contamination in the different soil layers. Thus, according to Pb maps, the majority of the investigation sites are green, implying that a significant part of the study areas was uncontaminated by Pb during the winter due to metals leaching into the lower part of the soil. Furthermore, the Ni maps 5–30 cm of soil were mostly pink, indicating that the soil was uncontaminated/moderately contaminated to moderately/strongly contaminated, but the upper portion of the soil was mostly green, denoting that the majority of the soil was uncontaminated by Ni.

According to the data, the I-geo values of three heavy metals were detected as non-polluted in highly polluted environments. In the different soil strata, the Cd, Pb, and Ni concentrations measured by I-geo vary significantly, Figs. 5–10. According to I-geo categorization, the Cd, Pb, and Ni varied from uncontaminated to extremely contaminated. The I-geo (Cd) exhibited a high accumulation influence in numerous samples, indicating high rates in the majority of samples during summer. In winter, there was also non-polluted soil in sample soil 6, as shown in Table 13.

These data suggest that the two soil layers in Erbil's Kani Qrzhala Subdistrict are rich in Cd, Cr, Ni, Cu, Pb, Zn, Hg, and Mn. The primary causes of soil contamination with Cd, Cr, Ni, Cu, Pb, Zn, Hg, and Mn are electronic products, electroplating waste, paint waste, spent batteries, etc.[44].

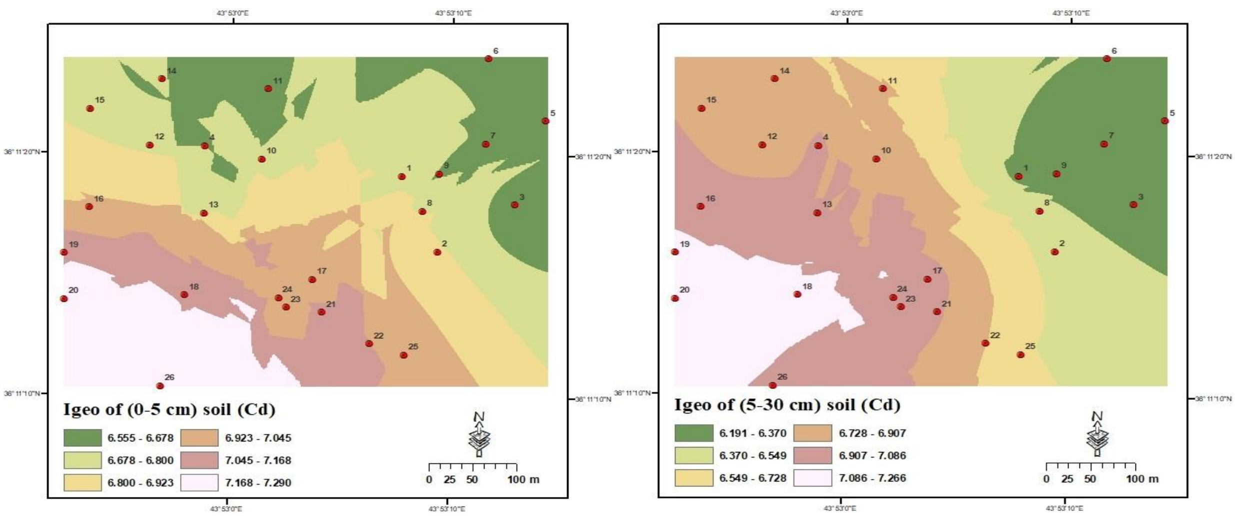

Figure 2. Spatial distribution of I-geo (Cd) in the two different layers of soils at study sites during summer.

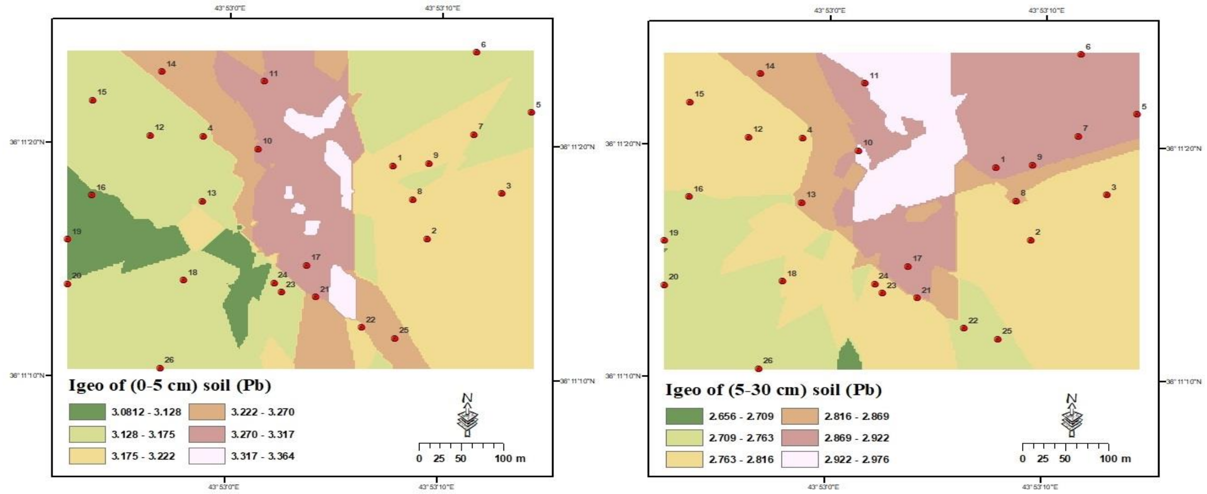

Figure 3. Spatial distribution of I-geo (Pb) in the two different layers of soils at study sites during summer.

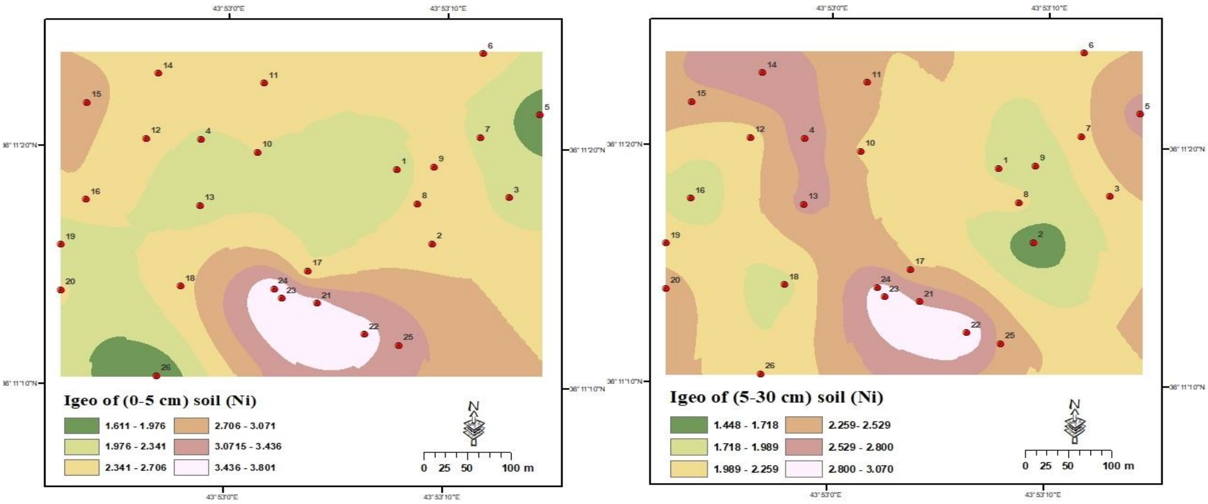

Figure 4. Spatial distribution of I-geo (Ni) in the two different layers of soils at study sites during summer.

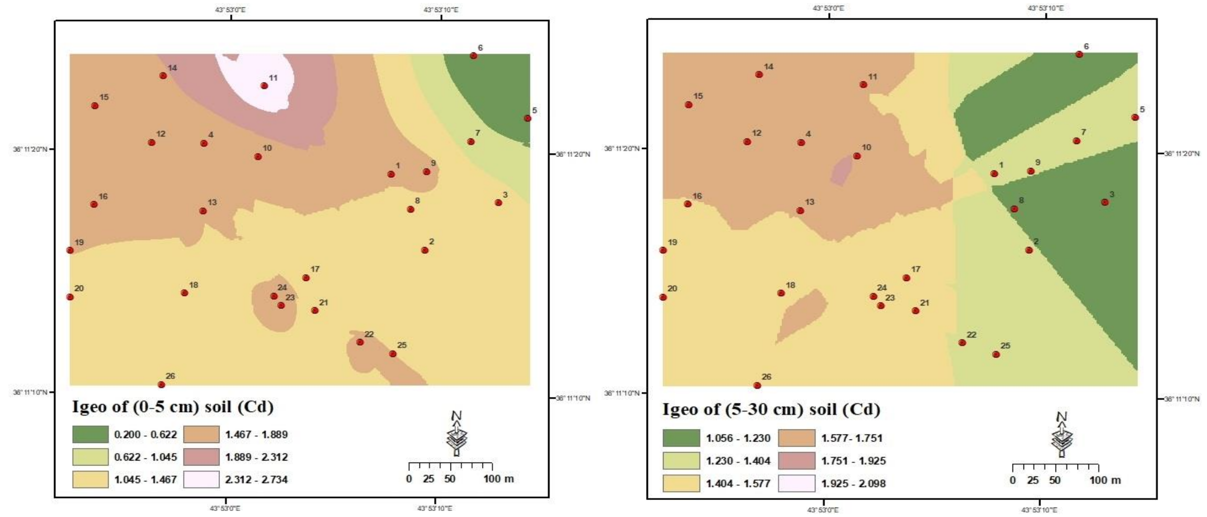

Figure 5. Spatial distribution of I-geo (Cd) in the two different layers of soils at study sites during winter.

2024, 21(3): 0867-0893
https://dx.doi.org/10.21123/bsj.2023.8382
P-ISSN: 2078-8665 - E-ISSN: 2411-7986
Baghdad Science Journal

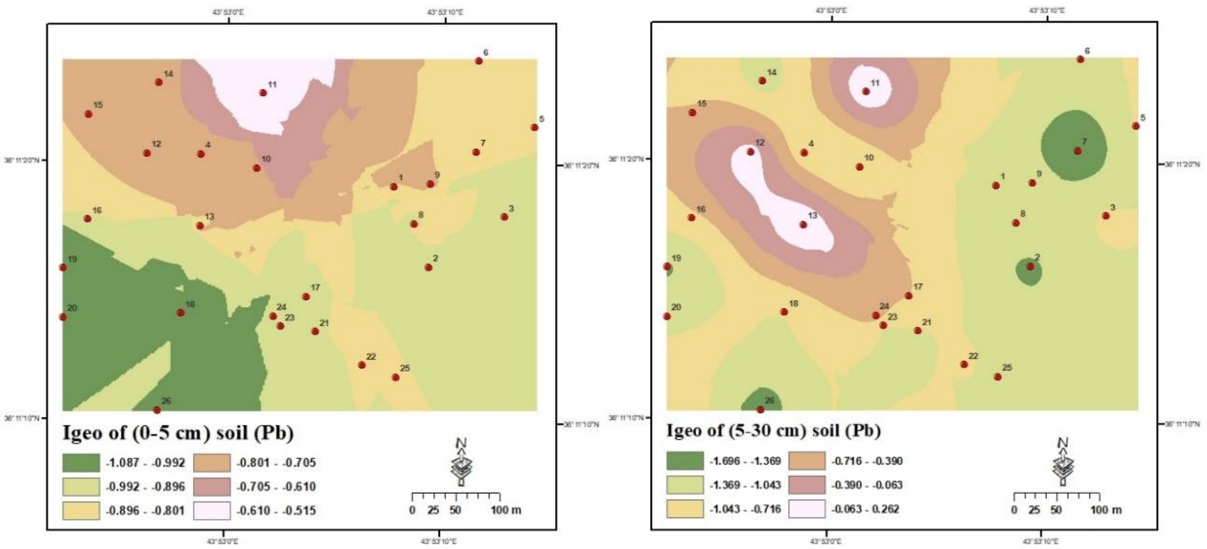

Figure 6. Spatial distribution of I-geo (Pb) in the two different layers of soils at study sites during winter.

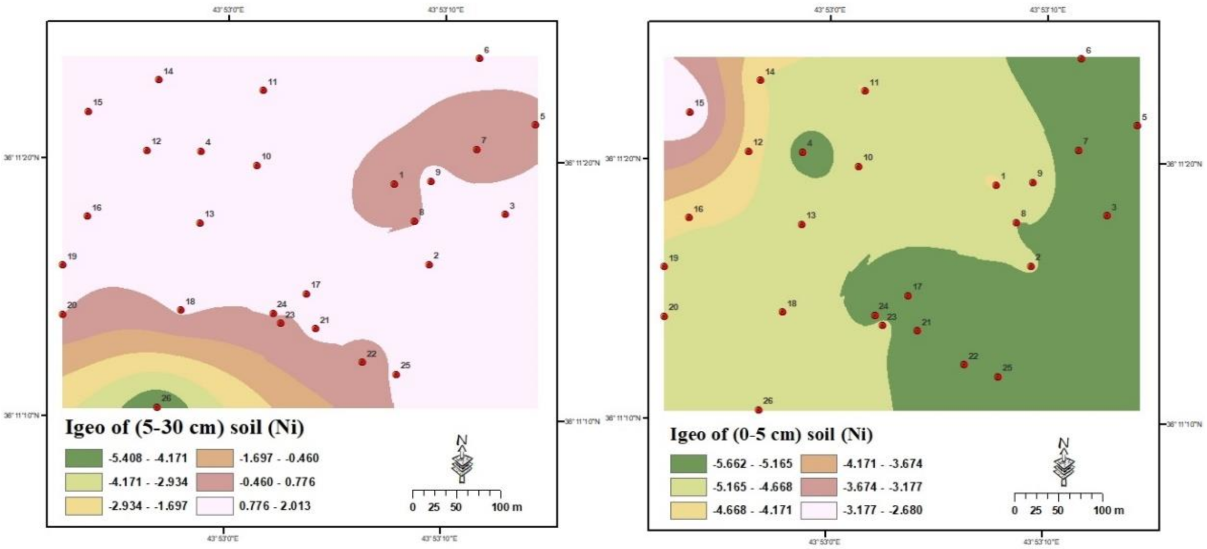

Figure 7. Spatial distribution of I-geo (Ni) in the two different layers of soils at study sites during winter.

Assessment of Contamination Risk Using Pollution Load Index:

Elsayed *et al.*,[45] developed the "pollution load index" (PLI) as a straightforward and proportional approach for determining the degree of heavy metal pollution. Hence, it is a unique indicator for comparing the level of pollution in various areas. The PLI outcomes, Figs. 8 and 9, were observed to be very high PLI > 1 for all of the analyzed samples during summer. Due to the influence of distinct outer causes of soil pollution, such as solid waste, industrial and agricultural operations, the PLI values for all samples are greater than one, denoting that the soil is extremely polluted [46].

Nevertheless, in winter, the pollution load index (PLI) was low in all samples, implying unpolluted soils because of cold temperatures, low activity of microorganisms, low chemical reactions, and rain-induced metal leaching into the lower soil layers [47], Figs. 10 and 11. The PLI value shows that the dry season soil samples contained more heavy metals than the wet season soil samples.

2024, 21(3): 0867-0893
https://dx.doi.org/10.21123/bsj.2023.8382
P-ISSN: 2078-8665 - E-ISSN: 2411-7986
Baghdad Science Journal

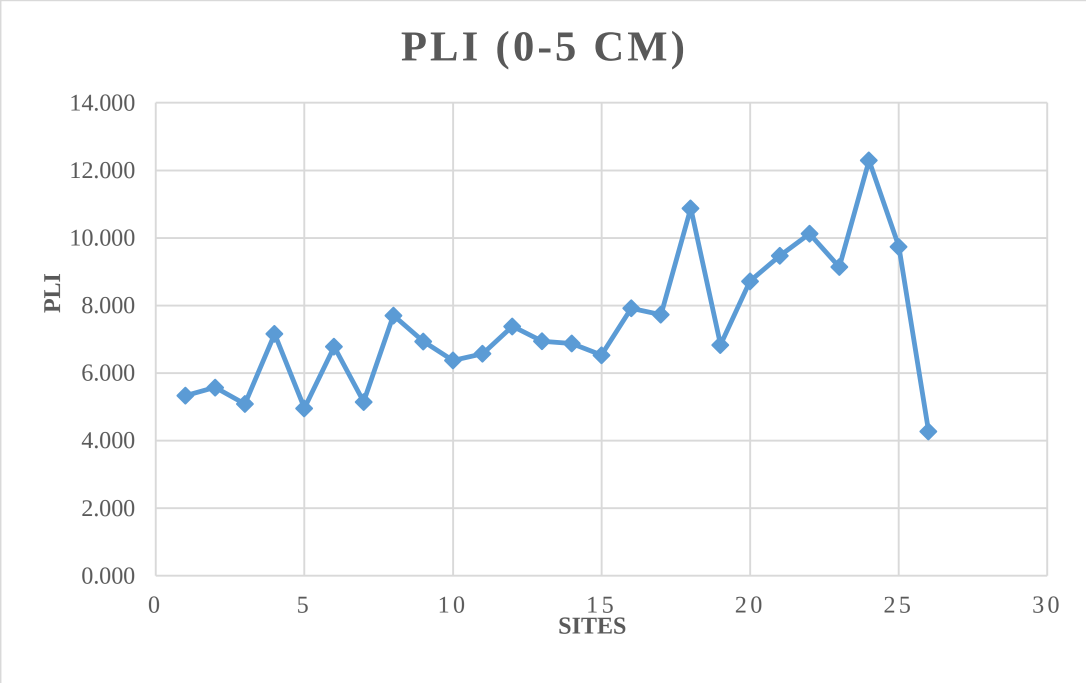

Figure 8. Pollution load index values and pollution levels in (0-5 cm) soil at study sites during summer.

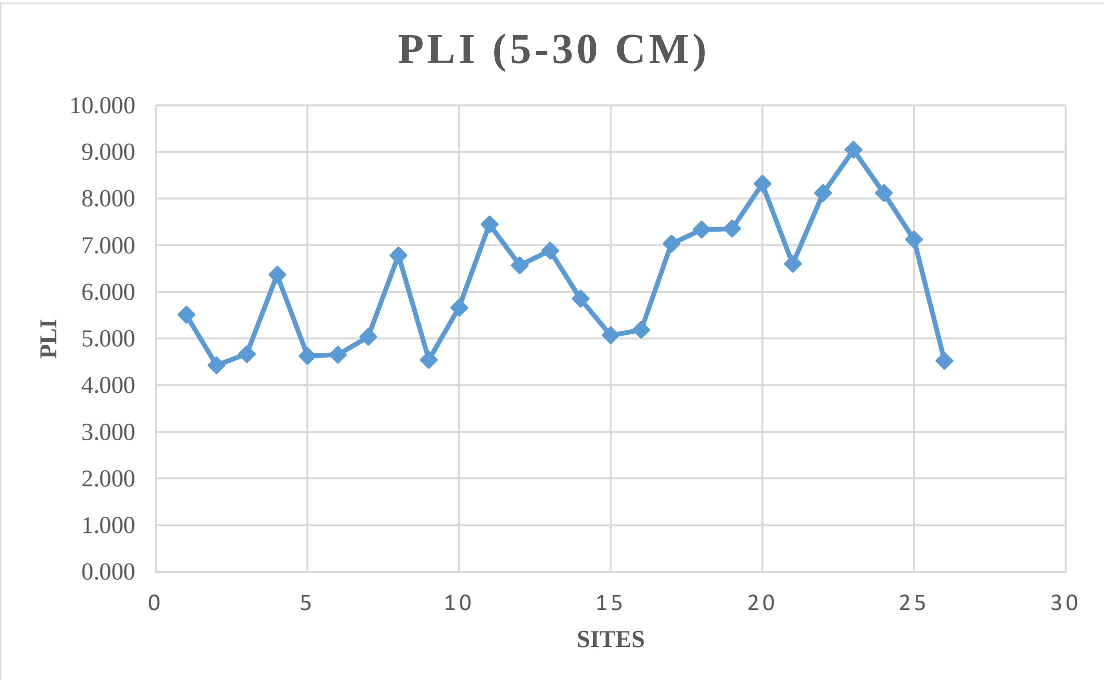

Figure 9. Pollution load index values and pollution levels in (5-30 cm) soil at study sites during summer.

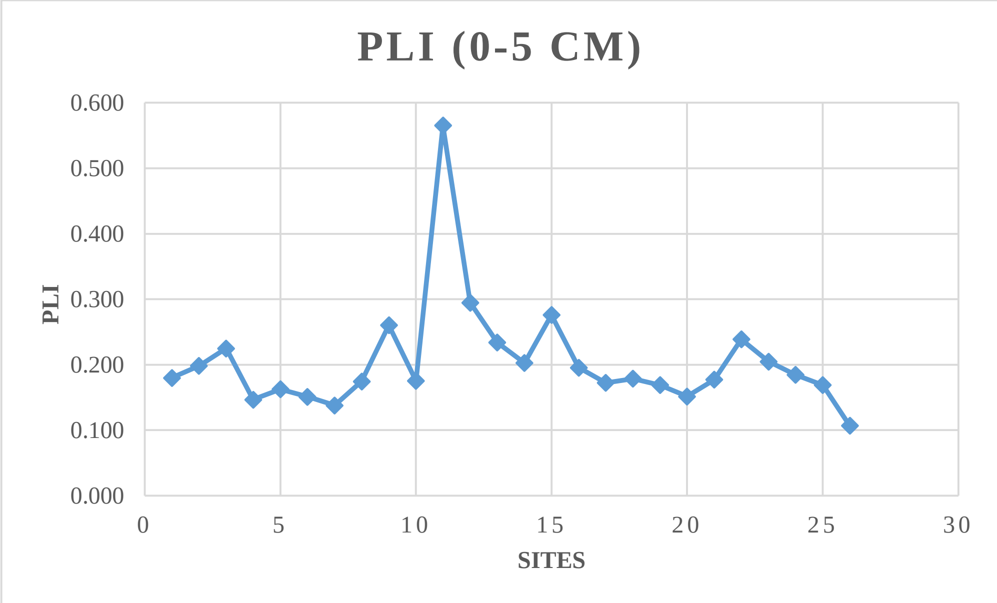

Figure 10. Pollution load index values and pollution levels in (0-5 cm) soil at study sites during winter.

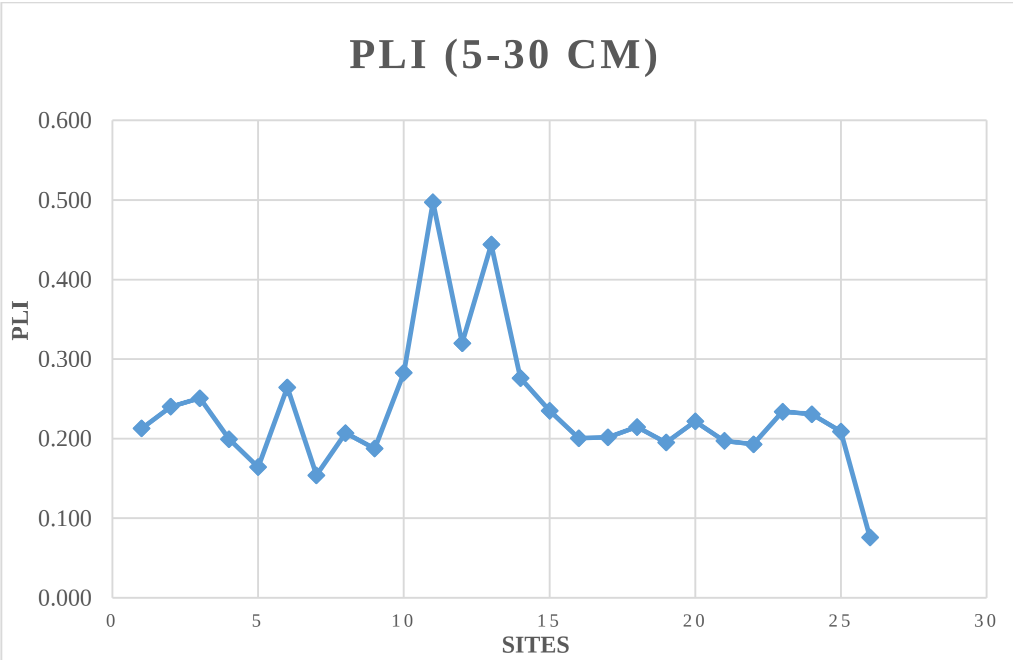

Figure 11. Pollution load index values and pollution levels in (5-30 cm) soil at study sites during winter.

Conclusion

This study reveals environmental contamination near the landfill site, emphasizing the importance of a comprehensive public health approach to deal with environmental contamination in local communities. Heavy elements were found in soils at the Erbil municipal waste landfill, including zinc, cadmium, lead, manganese, nickel, copper, chromium and mercury. Elements concentrations ranged as follows: Mn > Zn > Pb > Ni > Cr > Cu > Cd > Hg. Heavy element concentrations were generally highest at the landfill site. Furthermore, the soils at the landfill are highly contaminated with Mn (> 7000 mg kg^{-1}). The presence of metallic substances in the earth's crust, as well as Mn-containing waste, is attributed to the high level of Mn content in the soil. The findings indicated that a solid waste open dump site has a negative impact on soil quality in the study area and is a possible source of risk to human health via the food chain. According to the findings of this study, the soils surrounding the landfill are not suitable for agricultural activities due to heavy element leaching that may be picked up by food crops. These heavy element contaminants, however, were all below the allowable limits for agricultural soils. The EPA must conduct regular monitoring and raise awareness to ensure waste segregation prior to dumping in order to reduce elevated levels of contaminants (heavy elements) at the landfill, which may pose serious health risks. Alternatively, remediation technologies (for example, phytoremediation) could be introduced at the site to aid in the decontamination of the landfill area, particularly Mn. Eventually, it will be clear that a methodical and ongoing heavy element pollution control program is required, as well as other mitigation measures to reduce the rate and extent of pollution issues in the future.

Authors' Declaration

- Conflicts of Interest: None.
- We hereby confirm that all the Figures and Tables in the manuscript are ours. Furthermore, any Figures and images, that are not ours, have been included with the necessary permission for re-publication, which is attached to the manuscript.
- Authors sign on ethical consideration's approval.
- Ethical Clearance: The project was approved by the local ethical committee in University of Salahaddin.

Authors' Contribution Statement

S. Y. J. presented the concept, analysis, discussion of the findings, and manuscript writing. D. A. D. contributed to the research design and implementation, laboratory work. S. Y. J., and D. A. D. verified the analytical methods, discussed the results, and contributed to the final manuscript.

References

1. Mohamed EA, Abdelaziz BB, Enas EAE, Salah E. Assessment of Soil Pollution Levels in North Nile Delta, by Integrating Contamination Indices, GIS, and Multivariate Modeling. . Sustainability. 2021; 13(14): 1-20. https://doi.org/10.3390/su13148027.
2. Abd Alsammed SMZ. Advanced GIS-based Multi-Function Support System for Identifying the Best Route. Baghdad Sci J. 2022; 19(3): 0631-. https://doi.org/10.21123/bsj.2022.19.3.0631.
3. Wang J, Liu G, Liu H, Lam PK. Multivariate statistical evaluation of dissolved trace elements and a water quality assessment in the middle reaches of Huaihe River, Anhui, China. Sci Total Environ. 2017;583:421-31. https://doi.org/10.1016/j.scitotenv.2017.01.088.
4. Hu B, Jia X, Hu J, Xu D, Xia F, Li Y. International journal of engineering research and general scienceAssessment of heavy metal pollution and health risks in the soil-plant-human system in the Yangtze River Delta, China. Int J Env Res Public Health. 2017; 14(9): 1042. https://doi.org/10.3390/ijerph14091042.
5. Pourret O. On the necessity of banning the term "heavy metal" from the scientific literature. Sustainability. 2018;10(8):2879. https://doi.org/10.3390/su10082879.
6. Panagos P, Ballabio C, Lugato E, Jones A, Borrelli P, Scarpa S, et al. Potential sources of anthropogenic copper inputs to European agricultural soils. Sustainability. 2018; 10(7): 2380. https://doi.org/10.3390/su10072380.
7. Peter HR, Linda RB, George BJ. Environment. 2nd ed. Saunders College Publishing, New York, NY, USA1998. 9-12. https://doi.org/10.5897/AJAR2016.10907.
8. Shui L, Pan X, Chen X, Chang F, Wan D, Liu D, et al. Pollution characteristics and ecological risk assessment of heavy metals in sediments of the three gorges reservoir. Water. 2020; 12(6): 1798. https://doi.org/10.3390/w12061798.
9. Aziz SQ, Maulood YI. Contamination valuation of soil and groundwater source at anaerobic municipal solid waste landfill site. Environ Monit Assess. 2015; 187: 1-11. https://doi.org/10.1007/s10661-015-4971-y.
10. Bongoua-Devisme A, Bi EB, Kassin K, Balland-Bolou-Bi C, Gueable Y, Adiaffi B, et al. Assessment of heavy metal contamination degree of municipal open-air dumpsite on surrounding soils: Case of dumpsite of Bonoua, Ivory Coast. Int j eng res general sci. 2018; 6: 22-30. https://doi.org/ffhal-01891039f.

11. Makuleke P, Ngole-Jeme VM. Soil heavy metal distribution with depth around a closed landfill and their uptake by Datura stramonium. Appl Environ Soil Sci. 2020; 2020. https://doi.org/10.1155/2020/8872475.
12. Barbieri M, Sappa G, Nigro A. Soil pollution: Anthropogenic versus geogenic contributions over large areas of the Lazio region. J Geochem Explor. 2018; 195: 78-86. https://doi.org/10.1016/j.gexplo.2017.11.014
13. Lazem LF. Application of GIS technique in the studies on fish assemblages in Shatt Al-Arab River, Basrah, Iraq. Baghdad Sci J. 2022; 9 (4): 8-12. https://doi.org/10.21123/bsj.2022.19.4.0732.
14. Francini M, Artese S, Gaudio S, Palermo A, Viapiana MF. To support urban emergency planning: A GIS instrument for the choice of optimal routes based on seismic hazards. Int J Disaster Risk Reduct. 2018; 31: 121-34. https://doi.org/10.1016/j.ijdrr.2018.04.020.
15. Bing H, Wu Y, Zhou J, Sun H, Wang X, Zhu H. Spatial variation of heavy metal contamination in the riparian sediments after two-year flow regulation in the Three Gorges Reservoir, China. Sci Total Environ. 2019;649:1004-16. https://doi.org/10.1016/j.scitotenv.2018.08.401.
16. Natali C, Bianchini G. Natural vs anthropogenic components in sediments from the Po River delta coastal lagoons (NE Italy). Environ Sci Pollut Res. 2018; 25(3): 2981-91. https://doi.org/10.1007/s11356-017-0986-y.
17. Abowaly ME, Belal A-AA, Abd Elkhalek EE, Elsayed S, Abou Samra RM, Alshammari AS, et al. Assessment of soil pollution levels in North Nile Delta, by integrating contamination indices, GIS, and multivariate modeling. Sustainability. 2021; 13(14): 8027. https://doi.org/10.3390/su13148027.
18. Vongdala N, Tran H-D, Xuan TD, Teschke R, Khanh TD. Heavy metal accumulation in water, soil, and plants of municipal solid waste landfill in Vientiane, Laos. Int J Env Res Public Health. 2019; 16(1) :22. https://doi.org/10.3390/ijerph16010022.
19. Yilmaz G, Hocanli Y. Mapping of noise by using GIS in Şanliurfa. Environ Monit Assess. 2006; 121(1): 103-8. https://doi.org/10.1007/s10661-005-9109-1.
20. Bhunia GS, Shit PK, Maiti R. Comparison of GIS-based interpolation methods for spatial distribution of soil organic carbon (SOC). J Saudi Soc Agric Sci. 2018; 17(2): 114-26. https://doi.org/10.1016/j.jssas.2016.02.001.
21. Zhu H, Bing H, Wu Y, Zhou J, Sun H, Wang J, et al. The spatial and vertical distribution of heavy metal contamination in sediments of the Three Gorges Reservoir determined by anti-seasonal flow regulation. Sci Total Environ. 2019; 664:79-88. https://doi.org/10.1016/j.scitotenv.2019.02.016. .
22. Lu X, Wang L, Lei K, Huang J, Zhai Y. Contamination assessment of copper, lead, zinc, manganese and nickel in street dust of Baoji, NW China. J Hazard Mater. 2009; 161(2-3): 1058-62. https://doi.org/10.1016/j.jhazmat.2008.04.052.
23. Rahman SH, Khanam D, Adyel TM, Islam MS, Ahsan MA, Akbor MA. Assessment of heavy metal contamination of agricultural soil around Dhaka Export Processing Zone (DEPZ), Bangladesh: implication of seasonal variation and indices. Appl sci. 2012; 2(3): 584-601. https://doi.org/10.3390/app2030584.
24. Jorfi S, Maleki R, Jaafarzadeh N, Ahmadi M. Pollution load index for heavy metals in Mian-Ab plain soil, Khuzestan, Iran. Data br. 2017; 15: 584-90. https://doi.org/10.1016/j.dib.2017.10.017.
25. Karimi A, Naghizadeh A, Biglari H, Peirovi R, Ghasemi A, Zarei A. Assessment of human health risks and pollution index for heavy metals in farmlands irrigated by effluents of stabilization ponds. Environ Sci Pollut Res. 2020; 27(10): 10317-27. https://doi.org/10.1007/s11356-020-07642-6.
26. Jafari A, Ghaderpoori M, Kamarehi B, Abdipour H. Soil pollution evaluation and health risk assessment of heavy metals around Douroud cement factory, Iran. Environ Earth Sci. 2019;78(8): 1-9. https://doi.org/10.1007/s12665-019-8220-5
27. Wan D, Song L, Mao X, Yang J, Jin Z, Yang H. One-century sediment records of heavy metal pollution on the southeast Mongolian Plateau: Implications for air pollution trend in China. Chemosphere. 2019; 220: 539-45. https://doi.org/10.1016/j.chemosphere.2018.12.151.
28. Farid G, Sarwar N, Saifullah AA, Ghafoor A, Rehman M. Heavy metals (Cd, Ni and Pb) contamination of soils, plants and waters in Madina town of Faisalabad metropolitan and preparation of GIS based maps. Adv Crop Sci Tech. 2015; 4(2): 693-706. https://doi.org/doi:10.4172/2329-8863.1000199.
29. Xu M, Sun W, Wang R. Spatial distribution and ecological risk assessment of potentially harmful trace elements in surface sediments from Lake Dali, North China. Water. 2019; 11(12): 2544. https://doi.org/10.3390/w11122544.
30. Ferronato N, Torretta V. Waste mismanagement in developing countries: A review of global issues. Int J Env Res Public Health. 2019; 16(6): 1060. https://doi.org/10.3390/ijerph16061060.
31. Yan X, Liu M, Zhong J, Guo J, Wu W. How human activities affect heavy metal contamination of soil and sediment in a long-term reclaimed area of the Liaohe River Delta, North China. Sustainability.

2018; 10(2): 338. https://doi.org/10.3390/su10020338.
32. Peter T, Marina AT, Makafui AB, Adigun RA, Emmanuel O-T, Roseline O, et al. Assessment of the levels of cadmium and lead in soil and vegetable samples from selected dumpsites in the Kumasi Metropolis of Ghana. African J Agric Res. 2016; 11(18): 1608-16. https://doi.org/10.5897/AJAR2016.10907.
33. Dharmarathne N, Gunatilake J. Leachate characterization and surface groundwater pollution at municipal solid waste landfill of Gohagoda, Sri Lanka. Int J Sci Research. 2013; 3(11): 1-7. http://www.ijsrp.org/research-paper-1113.
34. Weggler K, McLaughlin MJ, Graham RD. Effect of chloride in soil solution on the plant availability of biosolid-borne cadmium. J Environ Qual. 2004; 33(2): 496-504. https://doi.org/10.2134/jeq2004.4960.
35. Agyarko K, Darteh E, Berlinger B. Metal levels in some refuse dump soils and plants in Ghana. Plant Soil Environ. 2010; 56(5): 244-51. https://doi.org/10.17221/13/2010-PSE.
36. Pasquini M, Alexander M. Chemical properties of urban waste ash produced by open burning on the Jos Plateau: implications for agriculture. Sci Total Environ. 2004; 319(1-3): 225-40. https://doi.org/10.1016/S0048-9697(03)00434-0.
37. Prasad S, Yadav KK, Kumar S, Gupta N, Cabral-Pinto MM, Rezania S, et al. Chromium contamination and effect on environmental health and its remediation: A sustainable approaches. J Environ Manage. 2021; 285: 112174. https://doi.org/10.1016/j.jenvman.2021.112174.
38. Cheng H, Hu Y. Mercury in municipal solid waste in China and its control: a review. Environ Sci Technol. 2012; 46(2): 593-605. https://doi.org/10.1021/es2026517.
39. Fahmida K, Rafizul Islam M, editors. Assessment of heavy metal contamination in soil of waste disposal site in Bangladesh: implication of spatial, seasonal variation and indices. G Civil Environ Sci Pollut Res Eng Con.; 2017: Springer. p. 6-18. https://doi.org/10.1007/978-981-10-8016-6_67.
40. Oluwatuyi OE, Ajibade FO, Ajibade TF, Adelodun B, Olowoselu AS, Adewumi JR, et al. Total concentration, contamination status and distribution of elements in a Nigerian State dumpsites soil. Environ Sustain Indic. 2020; 5: 100021. https://doi.org/10.1016/j.indic.2020.100021.
41. Kanmani S, Gandhimathi R. Assessment of heavy metal contamination in soil due to leachate migration from an open dumping site. Appl water sci. 2013; 3(1): 193-205. https://doi.org/10.1007/s13201-012-0072-z.
42. Quaghebeur M, Laenen B, Geysen D, Nielsen P, Pontikes Y, Van Gerven T, et al. Characterization of landfilled materials: screening of the enhanced landfill mining potential. J Cleaner Prod. 2013; 55: 72-83. https://doi.org/10.1007/s13201-012-0072-z.
43. Elbehiry F, Elbasiouny H, El-Ramady H, Brevik EC. Mobility, distribution, and potential risk assessment of selected trace elements in soils of the Nile Delta, Egypt. Environ Monit Assess. 2019; 191(12): 1-22. https://doi.org/10.1007/s10661-019-7892-3.
44. Shittu OS, Ayodele OJ, Ilori AO, Filani AO, Afuye AT. Heavy metal contamination of a dumpsite environment as assessed with pollution indices. Int J Agric Biosystems Eng. 2017; 12(1): 1-7. https://doi.org/Scholar.waset.org/1307-6892/10008346.
45. Elsayed S, Hussein H, Moghanm FS, Khedher KM, Eid EM, Gad M. Application of irrigation water quality indices and multivariate statistical techniques for surface water quality assessments in the Northern Nile Delta, Egypt. Water. 2020; 12(12): 3300. https://doi.org/10.3390/w12123300.
46. Liu R, Bao K, Yao S, Yang F, Wang X. Ecological risk assessment and distribution of potentially harmful trace elements in lake sediments of Songnen Plain, NE China. Ecotoxicol Environ Saf. 2018; 163: 117-24. https://doi.org/10.1016/j.ecoenv.2018.07.037.
47. Afolagboye LO, Ojo AA, Talabi AO. Evaluation of soil contamination status around a municipal waste dumpsite using contamination indices, soil-quality guidelines, and multivariate statistical analysis. SN Appl Sci. 2020; 2(11): 1-16. https://doi.org/10.1007/s42452-020-03678-y

2024, 21(3): 0867-0893
https://dx.doi.org/10.21123/bsj.2023.8382
P-ISSN: 2078-8665 - E-ISSN: 2411-7986
Baghdad Science Journal

التوزيع المكاني للعناصر الثقيلة في مكبات النفايات البلدية في أربيل باستخدام نظم المعلومات الجغرافية

سيران يوسف جلال، دلشاد عزيز درويش

قسم علوم البيئة والصحة، كلية العلوم، جامعة صلاح الدين، أربيل، العراق.

الخلاصة

إن إطلاق النفايات البلدية الصلبة غير المعالجة (MSW)على الأرض منتشر في البلدان النامية. لتقليل المستويات المرتفعة من المكونات الضارة في التربة الملوثة ، يلزم إجراء تقييم مناسب لتركيزات المعادن الثقيلة في مكب كاني قرزالة في أربيل بين آب / أغسطس 2021 وشباط / فبراير 2022. كان الغرض من هذه الدراسة فحص تأثير التخلص غير السليم من النفايات الصلبة على خصائص التربة داخل مكب النفايات من خلال تقييم مخاطر التلوث لثمانية عناصر الثقيلة في طبقتين منفصلتين من التربة باستخدام مؤشر التراكم الجغرافي (I-geo)ومؤشر حمل التلوث (PLI) المدعومين. تم استخدام برنامج ArcGIS لرسم خريطة التوزيع المكاني للتلوث عناصر الثقيلة والمخاطر البيئية المحتملة. أنتجت هذه الدراسة المؤشرات المذكورة أعلاه لثمانية عناصر ثقيلة ، بما في ذلك Zn و Cd و Pb و Mn و Ni و Cu و Hg. تشير هذه النتيجة إلى توزيع معنوي لـ I-geo Zn و Cd و Pb و Mn و Ni و Cu و Cr و Hg في كل من طبقات التربة. تباينت قيم I-geo في الصيف من -1.700 إلى 3.560 للزنك ، ومن 5.045 إلى 8.175 للقرص المضغوط ، ومن 2.318 إلى 4.329 للرصاص ، ومن 0 إلى 3.374 للمنغنيز ، ومن 1.439 إلى 3.880 للنيكل ، ومن 0.638 إلى 2.278 للنحاس ، ومن -0.541 إلى 2.665 لـ Cr ، و -2.495 إلى 0.778 للزئبق. بناءً على تصنيف Igeo ، تراوحت مستويات التلوث لـ Zn و Cd و Pb و Mn و Ni و Cu و Hg من غير ملوث إلى شديد التلوث. ومع ذلك ، تم تقييم جميع المعادن على أنها غير ملوثة طوال فصل الشتاء ، باستثناء I-geo (Cd) وI- geo (Ni) وتفاوتت من -0.467 إلى 3.966 و -5.720 إلى 2.015 مصنفة من غير ملوثة إلى قوية وغير ملوثة إلى معتدل / ملوثة بشدة على التوالي. وفقًا لفئة PLI ، تم تصنيف معظم العينات على أنها "شديدة التلوث" خلال فصل الصيف ، ولكن خلال موسم الأمطار ، تم تصنيف جميع العينات على أنها "غير ملوثة".

الكلمات المفتاحية: مؤشر التراكم الجغرافي، نظم المعلومات الجغرافية، عناصر الثقيلة، MSW، PLI.